

Reaction Kinetics of Cyanogen Iodide with Biological Thiols

By

Sbonelo Mkhize

Masters of Science



UNIVERSITY OF
KWAZULU-NATAL

INYUVESI
YAKWAZULU-NATALI

School of Chemistry and Physics

Pietermaritzburg

Reaction Kinetics of Cyanogen Iodide with Biological Thiols

A dissertation submitted to the University of KwaZulu-Natal fulfilling the academic requirements for the Degree of Master of Science

By

Sbonelo Mkhize

BSc (HONS) University of KwaZulu-Natal

School of Chemistry and Physics

University of KwaZulu-Natal

Pietermaritzburg

September 2021

Declaration

I hereby declare that the experimental work and results presented in this thesis are the original work of my study carried out in the School of Chemistry and Physics, University of KwaZulu-Natal, Pietermaritzburg campus and has never been submitted for the fulfillment of any degree at any institution.

..... 

Sbonelo Mkhize (Student)

I hereby certify that this is correct.

..... 

Dr. B.A. Xulu (Supervisor)

School of Chemistry and Physics

University of KwaZulu-Natal

Pietermaritzburg

September 2021

Dedications

I dedicate this work to my late mother and my entire family most importantly my young sister Zanele Mkhize for her encouragement, motivation and support she have showed me, which gave me the strength to fulfil this quest.

I thank the almighty God my source of inspiration and wisdom for surrounding me with most warm hearted-people.

Abstract

In biological fluids such as the saliva, the interpseudoalogen cyanogen iodide (ICN) is produced in the presence or absence of human peroxidases. A mixture of chemical species with antimicrobial properties is produced in the presence of both I^- and SCN^- depending upon the pH of the reaction. The mixture of transient and stable chemical species includes $I_2/I_3^-/HOI/OI^-/ICN$. Cyanogen iodide is a potent antimicrobial agent that is at least 1000 times more effective in killing bacteria than hypothiocyanite ($OSCN^-$), an exclusive oxidation product of all defensive peroxidases in saliva. It is a chemically stable product that can accumulate over time in the oral cavity with a half-life of about 16.9 years at pH 7. Our experiments capitalize on the discovery that one ICN is produced stoichiometrically for every four I_2 molecules that react with SCN^- . This study shows that $OSCN^-$ oxidizes I^- to I_2 (via HOI/OI^- intermediate) which subsequently reacts with SCN^- to produce ICN. The formation of the intermediate HOI/OI^- (345 nm) was confirmed using the stopped-flow spectroscopy. The UV-visible spectrum of ICN contains an absorbance band at 222 nm. ^{13}C -labelled SCN^- , ^{13}C NMR spectroscopy and mass spectrometry further confirmed the presence of ICN. Here we report for the first time the second-order rate constants for the reaction of ICN with selected biological thiols and some preliminary tests on the antimicrobial activity of ICN. The reactions of ICN with thiols occur with second-order rate constants in the range from $10^2 - 10^5 M^{-1} s^{-1}$ at pH 6 - 7.4 as determined by stopped-flow spectroscopy. The rate constant for the reaction of ICN with a protein-bound thiol (BSA) was also determined by competition kinetics. ICN reacts with BSA with a second-order rate constant of $130 M^{-1} s^{-1}$ at pH 7.4. The rate of ICN reaction with thiols show an inverse relationship against the pKa of the thiol group. These kinetic rate constants together with the results

of antimicrobial studies (against *E.coli*) indicate that ICN plays a key antimicrobial role in the oral cavity and other biological fluids.

Table of contents

Contents

Acknowledgments.....	i
List of Abbreviations.....	iii
List of Figures.....	vi
List of Tables.....	viii
List of Schemes.....	ix
Chapter 1.....	1
1. Introduction.....	1
1.1. Problem Statement.....	1
1.2. Aims and Objectives.....	2
1.3. General background.....	3
1.4. Halogen-based antimicrobial.....	4
1.5. Oxidative burst.....	7
1.6. Relevant studies on the reaction of hypo(pseudo) halides with biological groups.....	9
1.6.1. Kinetics of the reaction of OSCN ⁻ with thiols.....	9
1.7. Antimicrobial studies of ICN.....	12
1.8. References.....	13
Chapter 2.....	22
2. Experimental Procedures.....	22
2.1. Reagents and Buffer Solutions.....	22
2.1.1. Iodine preparation.....	23
2.1.2. Synthesis of cyanogen iodide (ICN).....	23
2.2. Instrumentation.....	24
2.2.1. UV-Vis spectroscopy.....	24
2.2.2. pH Measurements.....	25
2.2.3. Stopped-flow studies.....	25
2.2.4. Mass Spectrometry.....	25
2.2.5. ¹³ C NMR Measurements.....	26
2.2.6. Infrared (IR) Spectroscopy.....	26
2.3. Competition kinetic studies.....	26
2.4. Antimicrobial studies.....	27
2.5. Reference.....	28
Chapter 3.....	29
3. Results and Discussion.....	29

3.1.	Production of ICN via a non-enzyme system	29
3.1.1.	Reaction of I^- with $OSCN^-$ to form I_2	29
3.1.2.	Reaction of I_2 with SCN^- to produce cyanogen iodide (ICN).....	32
3.2.	Synthesis of 5-thio-2-nitrobenzoic acid (TNB)	35
3.3.	Synthesis of cyanogen iodide (ICN).....	37
3.4.	Characterization of cyanogen iodide (ICN)	38
3.5.	Oxidation of selected biological thiols by ICN.....	44
3.5.1.	Reaction of ICN with TNB.....	44
3.5.2.	Reaction of ICN with selected biological thiol groups	46
3.5.3.	Reaction of ICN with thiol-bearing proteins	51
3.5.4.	Factors influencing the observed rate constants.....	52
3.5.4.1.	pH dependence of ICN reactions	52
3.5.4.2.	Dependence of the reactivity on thiol pKa	52
3.6.	Preliminary investigation of ICN antimicrobial activity	54
3.7.	Conclusion.....	56
3.8.	Reference	57
Appendix 1	59

Acknowledgments

I would like to express my deepest gratitude to my supervisor Dr. B.A Xulu for believing in me and letting me to be part of his research group and for his assistance and guidance throughout this research project.

I also wish to express my appreciation to the following people:

- **Thabani Xulu** for mentoring and training me on how to use the stopped-flow and most importantly on how to analyse the kinetics data.
- To my previous research group members **Thabani Xulu, Nkosingizwile Xulu, Mabulala Mnguni** and to my current research member **Nomaswazi Madonsela** for their support, assistance and lab work training.
- To my colleagues Chem 8 for encouragement and support.
- **Dr. A Mambanda** for proofreading and giving constructive feedback.
- Physical chemistry staff **Dr. D Reddy** and **Dr. R.T Papo** for all the support they have given to me with regards to instruments.
- **Nkosingizwile Xulu** for always listening to my problems and offering good advices all the time.
- To my family including my late mother for their prayers, unconditional love and encouragement. Without their support this study work would not have been possible.
- To all my friends in the department of chemistry for their continuous support and encouragement.

Last but not least, I am thankful to everyone who took part in making this thesis real

I would also like to acknowledge:

- **Mr. Craig Grimmer** and **Mrs. Caryl J. Van Rensburg** for their assistance with NMR and Mass spectra analysis respectively.
- The NRF (National Research Foundation) of South Africa for their financial support.
- All the technical staff in the department of chemistry for their assistance

List of Abbreviations

I ₂	Iodine
I ⁻	Iodine ion
Cl ⁻	Chloride ion
Br ⁻	Bromide ion
KI	Potassium iodide
ICN	Cyanogen iodide
NaCN	Sodium cyanide
SCN ⁻	Thiocyanate ion
OSCN ⁻	Hypothiocyanite ion
H ₂ O ₂	Hydrogen peroxide
HOI	Hypoiodous acid
TNB	5-thio-2-nitrobenzoic acid
DTNB	5,5'-dithiobis(2-nitrobenzoic acid)
SPO	Salivary peroxidase
LPO	Lactoperoxidase
MPO	Myeloperoxidase
GSH	Glutathione
Cys	Cysteine

Cys MeE	L-Cysteine methyl ester
Nac	<i>N</i> -Acetyl-cysteine
Pen	Penicillamine
BSA	Bovine Serum Albumin
CK	Creatine kinase
HCl	Hydrogen chloride
NaOH	Sodium hydroxide
UV-Vis	Ultraviolet–visible
NMR	Nuclear magnetic resonance
FT-IR	Fourier-transform infrared
TOF-MS	Time-of-flight mass spectrometry
λ_{\max}	Maximum absorbance
ϵ	Molar absorptivity
$^{\circ}\text{C}$	Degrees Celsius
rt	Room temperature
$\text{NaH}_2\text{PO}_4 \cdot 2\text{H}_2\text{O}$	Sodium phosphate monobasic dehydrate
Na_2HPO_4	Sodium phosphate dibasic
NaOCl	Sodium hypochlorite
HOCl	Hypochlorite acid
HOBr	Hypobromous acid

OI^- Hypiodite

NaI Sodium iodide

List of Figures

Figure 1: Time resolved spectra showing the formation of hypiodite ion (OI ⁻) and the disappearance of OSCN ⁻	30
Figure 2: Kinetic trace for the formation and decomposition of HOI between 280-345 nm.	31
Figure 3: Time resolved spectral changes showing the formation of ICN in distilled water.	32
Figure 4: Kinetic trace showing the formation of ICN at 222 nm over time.	33
Figure 5: ¹³ C NMR spectra for the reaction of I ₂ with S ¹³ CN in deionized water.....	34
Figure 6: The UV-Vis spectra of TNB in phosphate buffer at pH 7.4.	36
Figure 7: The UV-Vis spectrum of ICN, maximum absorption at 222 nm, $\epsilon = 179 \text{ M}^{-1} \text{ cm}^{-1}$	38
Figure 8: ¹³ C NMR spectrum of ICN.	39
Figure 9: Mass spectrum of ICN in the positive ion mode.	40
Figure 10: Accurate mass spectrum of ICN in the positive ion mode.	41
Figure 11: FT-IR spectrum of ICN.	42
Figure 12: Raman spectrum of ICN.	43
Figure 13: Time-resolved spectral changes observed after reacting ICN (10 μM) with TNB (50 μM).....	44
Figure 14: Typical kinetic trace showing the disappearance of TNB at 412 nm over time.	45
Figure 15: Linear plot for the observed rate constants k_{obs} following the disappearance of TNB at 412 nm. Result are represented as mean standard deviation. Some error bars are smaller than the size of the symbol.	46
Figure 16: Kinetic traces showing the loss of TNB absorbance with increasing concentrations of the competing thiol L-cysteine at 412 nm.....	48

Figure 17: Plot of the linear analysis for the competitive kinetic data for L-cysteine with ICN at 412 nm. Result are represented as mean standard deviation. Some error bars are smaller than the size of the symbol. 49

Figure 18: The linear plot showing the relationship between the second-order rate constants and thiol pKa for the reaction of thiols with ICN at pH 7.4. ⁸..... 53

Figure 19: The agar plates taken before and after placing the plates under the fume hood cardboard. (A₁) Control with no *E. coli*; (B₁) with glycerol; (C₁) with KI; (D₁) with ICN. The agar plates taken after 30 days. (A₂) Control with no *E. coli*; (B₂) with Glycerol; (C₂) with KI; (D₂) with ICN. 55

Figure 20: Linear plot for the observed rate constants k_{obs} following the disappearance of TNB at 412 nm..... 59

Figure 21: Plot of the linear analysis for the competitive kinetic data for L-cysteine with ICN at 412 nm. 60

List of Tables

Table 1: The second-order rate constants for thiols starting from low-molecular mass to high-molecular mass or macro-thiols (proteins). ⁵⁹	10
Table 2: The second-order rate constants in 0.1M phosphate buffer (pH 7.4) at 22 °C, for the reaction of ICN with low-molecular-mass thiols.....	50

List of Schemes

Scheme 1: Formation of TNB from the reduction of DTNB.....	35
Scheme 2: Synthetic pathway for ICN.	37

Chapter 1

1. Introduction

1.1. Problem Statement

Microbial infections are an emerging and escalating challenge for public health globally. The new resistance mechanisms to antibiotic drugs exhibited by microorganism such as bacteria, fungi, viruses and parasites severely by limits effort to prevent and treat infections. In the 2014 report titled “Antimicrobial resistance: global report on surveillance” the world health organization (WHO) note a rise in the number of life-saving drugs that are rendered ineffective by resistance against serious diseases such as such tuberculosis, malaria and human immunodeficiency virus. ¹

The burden added by antibiotic-resistant infections is often reflected in higher healthcare costs for patients with resistant infections than for patients with non-resistant infections. Alarming statistics reveal that in the year 2013, infections claimed approximately 9.2 million lives i.e. about 17% of total deaths worldwide. ² In the United States alone, the centers for disease control and prevent (CDC) estimates the annual infection cases at about 2.8 million, of which approximately 35 000 people subsequently die every year. Consequently, WHO has identified microbial infections as a serious threat to global health.

1.2. Aims and Objectives

In this study, kinetic data for the reactions of cyanogen iodide (ICN) with biological thiols was collected using the stopped-flow system. Furthermore, preliminary experiments to test the activity of ICN were conducted against *Escherichia coli* (*E. coli*). The specific objectives were to:

- Synthesis and characterization of cyanogen iodide using the literature methods.
- Determine the second-order rate constants for the reactions of ICN with thiols,
- Preliminary tests on the activity of ICN against *E. coli*.

1.3. General background

Antimicrobials are agents used to inhibit the growth of or to kill disease causing microorganisms such as bacteria, fungi, parasites and viruses in living systems. ⁴⁻⁵ Human defensive peroxidases play a central role to facilitate the production of antimicrobials. They employ hydrogen peroxidase (H_2O_2) as an oxidant of small inorganic ions, resulting in the production of antimicrobials that are generally more effective than H_2O_2 itself. ⁶⁻⁸ Thiocyanate (SCN^-) is generally regarded the preferred substrate of and hypothiocyanite (OSCN^-) the only product of all defensive peroxidases in the saliva. ⁹⁻¹¹ Interestingly, despite the fact that all human defensive peroxidases can utilize iodide as a substrate, the involvement of I^- in the host defense has largely been ignored. ⁸

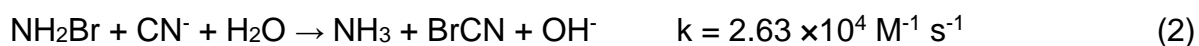
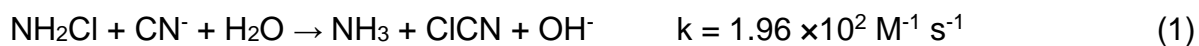
The basis for ignoring possible involvement of I^- in host defense is its scarcity in most physiologic fluids due to sequestering in the thyroid gland. However, more studies challenging this conclusion are emerging in the literature. ¹²⁻¹³ This work reports on non-enzymatic reactions that generate ICN and its kinetic reactions with selected physiologic thiol groups.

1.4. Halogen-based antimicrobial

Cyanogen halides ($X-CN$, $X = Cl, Br, I$) are a group of colourless, volatile and highly cytotoxic compounds. These interseudohalogenes are very irritating to the eyes and respiratory tract at very low concentrations in the atmosphere. ¹⁴⁻¹⁸ They are also known as asymmetric pseudohalogenes and while $BrCN$ and $ClCN$ are the most studied; information about ICN is poorly reported. They are strong oxidizing agents and are highly reactive because the pseudohalogen bond is weak. Both $ClCN$ and $BrCN$ are disinfection byproducts that are found in ozone free chlorinated and monochlorine treated drinking water. ¹⁹⁻²² Among the several reactions proposed for their formation in drinking water, the pathways initiated by the reaction of monochloramine (NH_2Cl) and monobromamine (NH_2Br) with formaldehyde ($HCHO$) are the most reported. The reaction of NH_2Br forms $BrCN$ following a parallel reaction of $ClCN$ formation. In addition to formaldehyde, other reactions involving humic acids, amino acids, proteins and peptides, and purines also lead to $ClCN$ formation. ²³⁻²⁶

Furthermore, cyanogen chloride ($ClCN$) can be produced as a toxic disinfection by-product of the reaction of free chloramines or chlorine with natural organic matter. ²⁷ $ClCN$ can also be produced from the enzyme-based reaction of HCN with H_2O_2-Cl in the presence of myeloperoxidase enzyme. ²⁸ This cyanogen halide can oxidize low molecular thiols at neutral pH. In addition, it can react with the bovine serum albumin (BSA) of the bacterium *Staphylococcus epidermis* specifically targeting the thiol groups. ¹⁴ $BrCN$ has been reported to cleave carbon-heteroatoms of tertiary amines into organo-cyanomides in the von Braun reaction. ²⁹ It is a well-known cleaving reagent of specifically the proteins. Furthermore, $BrCN$ is also used in the detection of pyridine compounds. ^{16-17, 29}

The second-order rate constant for the formation of ClCN and BrCN monochloramine and monobromamine have been reported. These reactions were studied at 25 °C and an ionic strength of 0.10 M NaClO₄ using the stopped-flow technique.³⁰⁻³¹



The rate constants for the formation of ClCN, BrCN and ICN were further determined from the reaction of hypohalous acids (HOCl, HOBr and HOI) with cyanide (CN⁻) as 310 M⁻¹ s⁻¹, 5.7 ×10⁷ M⁻¹ s⁻¹ and 6.0 ×10⁷ M⁻¹ s⁻¹ respectively at 25°C and an ionic strength of 1.00 M NaClO₄.³²



Pseudohalogens (ClCN, BrCN and ICN) eventually decomposes through a hydroxide-catalyzed hydrolysis pathway to produce cyanate ion.^{27, 32}



In the field of study of human defensive peroxidases, it is generally assumed that iodine from which ICN is produced is only present in trace amounts in most physiological fluids.³³ This assumption has led to the possible role of iodine in host defense being largely ignored.

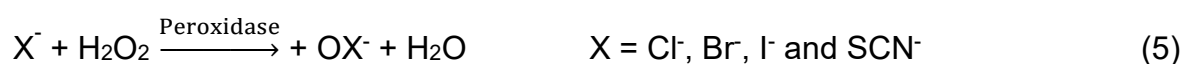
Iodine is an essential element in the production of thyroid hormones that regulate growth and metabolism. Humans rely heavily on dietary sources for iodine intake. Approximately 15-20 mg is found in a healthy human body and about 70-80 % of this amount is found in the thyroid gland.³⁴⁻³⁸ The biological role of halides such as Cl⁻ and Br⁻ and pseudo halide (SCN⁻) in human inflammatory diseases is extensively reported

while that of iodide (I^-) beyond the synthesis of thyroid hormones is not well understood.

Recent studies have reported that iodide (I^-) plays an important role in the chemistry of the oral cavity.^{12-13, 39} This suggests that iodine (I^- , I_2) in the oral cavity can react with thiocyanate via both the enzyme catalyzed and non-enzymatic reactions to produce the interpseudoalogen cyanogen iodide (ICN).^{12, 15} The oral cavity is known to produce trace amounts of ICN from the reaction of iodine (I_2) with thiocyanate (SCN^-). ICN is believed to be one of the naturally active antimicrobials in the oral cavity of mammals, responsible for fighting against dental bacteria and formation of tooth decay. The non-enzymatic reaction are believed to be major contributors as they provide a variety of pathways through which ICN can be formed.

1.5. Oxidative burst

Neutrophils are cells that provide the first line in host defense against invading foreign substances including bacteria, fungi and viruses. The redox chemistry of halide-derived oxidants produced by enzyme (peroxidase)-catalyzed reactions and non-enzymatic secondary reactions play a crucial role in human health and diseases.⁷ The peroxidase system consist of an enzyme (e.g. LPO)/ substrate (e.g. halide or pseudo-halide) and hydrogen peroxide.⁸ The hypo(pseudo)halides (OCl^- , OBr^- , OI^- and OSCN^-) are primary products of enzyme-catalyzed reactions possessing antimicrobial properties.⁴⁰⁻⁴²

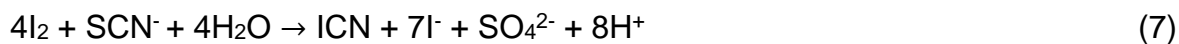


Hypo(pseudo)halides are powerful oxidants that are capable of modifying lipids, proteins, nucleic acids and of consuming antioxidants such as glutathione.⁴³⁻⁴⁴ Literature evidence suggests that OSCN^- is the only product of defensive peroxidases mammalian fluids such as saliva, milk, tears and mucus.^{8, 45-47} This is a result of thiocyanate generally being regarded a preferred substrate for peroxidases over the halogens.^{6, 41, 48-49} Hypothiocyanite ions (OSCN^-) is unstable and is short-lived (pKa 5.3 for HOSCN) and specifically targets thiol groups.^{12, 42, 50-51} Although all of the peroxidases can utilize iodide (I^-) as a substrate; its contribution in host defense has been overlooked due to scarcity of I^- in most physiological fluids. However, high concentration of I^- in the mucosal layer of the lung which also contains large amounts of lactoperoxidase (LPO) has been credited for reduced lung infection.⁵² In the

presence of I⁻, SCN⁻, H₂O₂ and lactoperoxidase, ICN which is at least 1000 times more effective in killing bacteria than OSCN⁻ is produced. ¹²



The inter (pseudo)halogen (ICN) is thus predicted as the most effective I⁺ antimicrobial under physiological conditions. The activity of ICN has recently been demonstrated against *Escherichia coli* (*E. coli*) bacteria. ¹³ Unlike OSCN⁻, ICN has a much longer half-life of 16.9 years at pH 7 and therefore can accumulate with time in specific fluids where they are generated. ¹² It is proposed in this work that non-enzymatic secondary reaction play a more significant role in the production of ICN and other iodide-based products. It has been known for more than hundred years now that ICN is stoichiometrically produced when I₂ reacts with SCN⁻. ¹⁵



1.6. Relevant studies on the reaction of hypo(pseudo) halides with biological groups

1.6.1. Kinetics of the reaction of OSCN⁻ with thiols

Sulfur-containing compounds commonly known as thiols (free and protein-bound) are preferred targets of hypo(pseudo) halides.^{11, 53} These reactions often result in permanent modifications to protein structure and disruptions to redox-regulated processes.^{6, 11, 54-57} While the hypohalides (HOCl, HOBr, and HOI) are highly reactive towards a variety of biological molecules, HOSCN predominantly reacts with thiols.¹¹ Studies on the reaction of thiols with hypo(pseudo)halides have shown that disulfides are common oxidation products of these reactions.⁵³ However, other studies have also reported that thiols can be oxidized to sulfenic (RSOH), sulfinic (RSO₂H), sulfonic (RSO₃H) acid forms under certain conditions and disulfides can be further oxidized to thiosulfinate ester (RO(O)SR) and thiosulfonate ester-(RS(O₂)SR).^{48, 58} The reported kinetic data of thiol oxidation by hypo(pseudo)halides reveals that HOSCN reacts rapidly with thiols, with rate constants ranging from 10³ – 10⁶ M⁻¹ s⁻¹, see Table 1.⁵⁹

Table 1: The second-order rate constants for the reaction of HOSCN with low-molecular mass to high-molecular mass or macro-thiols (proteins).⁵⁹

Substrate	pH	k_2 (HOSCN) ($M^{-1} s^{-1}$)	
2-nitro-5-thiobenzoate (TNB)	7.4	$(3.8 \pm 0.2) \times 10^5$	
	6.7	$(1.62 \pm 0.03) \times 10^6$	
	6.0	$(7.7 \pm 0.9) \times 10^6$	
L-Cysteine	7.4	$(7.8 \pm 1.4) \times 10^4$	
Cysteamine	7.4	$(7.1 \pm 0.7) \times 10^4$	
N-Acetyl-cysteine	7.4	$(7.3 \pm 1.6) \times 10^3$	
L-Cysteine methyl ester	7.4	$(1.6 \pm 0.1) \times 10^5$	
Penicillamine	7.4	$(3.0 \pm 0.7) \times 10^5$	
GSH	7.4	$(2.5 \pm 0.4) \times 10^4$	
	6.7	$(3.1 \pm 0.3) \times 10^4$	
	6.0	$(4.0 \pm 0.4) \times 10^4$	
BSA, thiol-containing proteins	7.4	$(7.6 \pm 1.5) \times 10^4$	
	Creatine kinase	7.4	$(3.1 \pm 0.6) \times 10^4$
	β-Lactoglobulin	7.4	$(1.0 \pm 0.1) \times 10^4$
	β-L-Crystallins	7.4	$(1.4 \pm 0.1) \times 10^4$

Furthermore, studies shown that HO₂SCN induces more cell apoptosis than hypohalides due to its targeting of specific important thiol groups.⁶⁰ The reactivity of thiols with hypo(pseudo) halides vary substantially and show an inverse dependence to the pK_a of the thiol group.⁶¹ Cyanogen iodide (ICN) is highly cytotoxic and its antimicrobial activity has been described against bacteria such as *Escherichia coli* (*E. coli*); *Fusobacterium nucleatum*, *Candida albicans* and *Staphylococcus aureus*.⁶²⁻⁶³ Despite the potential importance of ICN as an antimicrobial agent, on kinetic data for its reaction with physiological thiols are not available in the literature.

A recent study has demonstrated that haem proteins lactoperoxidase (LPO) and myeloperoxidase (MPO) both form ICN in the presence of I⁻, SCN⁻, and H₂O₂.¹² The formation of ICN by both the enzyme and non-enzymatic suggest possible involvement in host defense. Furthermore, the extended application of ICN as a preservative in food, oral care and cosmetic products requires knowledge of the rate constants of its reactions with biological molecules such as thiols. If the rate of the reaction of ICN with thiols are slow then its formation reduces potential host damage through the formation of a relatively milder oxidant. If however the reaction rates are fast, then the reaction with thiols is likely the pathway through which it executes antimicrobial activity. The second-order rate constants for ICN with physiological thiols were determine by competition experiments using 5-thio-2-nitrobenzoic acid (TNB). Competition experiments were used because physiological thiols do not have unique spectral signatures and ICN exhibits a low molar extinction coefficient ($\epsilon_{222\text{ nm}} = 179\text{ M}^{-1}\text{ cm}^{-1}$).

1.7. Antimicrobial studies of ICN

Antimicrobial resistance is a major challenge in medicinal applications and in the food production industry. ^{1, 65-66} Therefore, new antimicrobial agents that are iodine-based are required. These iodine-based antimicrobials (such as ICN) likely play a key role in controlling bacterial growth in the oral cavity and in the mucosal lining of the lungs where both iodine and thiocyanate are present. In the presence of a peroxidase enzyme, I^- and SCN^- compete for oxidation by H_2O_2 . ⁶⁷⁻⁶⁸ These reactions are pH sensitive and often result in a mixture of various species with antimicrobial properties. The reaction products of these oxidation reactions have not been characterized in details. A more recent study carried out by Bafort and co-workers describes the formation of diiodothiocyanate (I_2SCN^-) and dithiocyanate iodide ($I(SCN)_2^-$) by the lactoperoxidase catalysed reaction, and from the reaction between ICN and SCN^- . ⁹ The biological activity of I_2SCN^- was confirmed against *Penicillium expansum*.

1.8. References

1. Organization, W. H. *Antimicrobial resistance global report on surveillance: 2014 summary*; World Health Organization: **2014**.
2. Khameneh, B.; Iranshahy, M.; Soheili, V.; Bazzaz, B. S. F., Review on plant antimicrobials: A mechanistic viewpoint. *Antimicrobial Resistance & Infection Control* **2019**, *8* (1), 118.
3. Control, C. F. D.; Prevention, Biggest Threats and Data 2019 AR Threats Report. **2019**.
4. Ahmad, S.; Dar, M. I.; Pharm, B., Antibiotics and preventing their misuse. *Physicians Academy* **2011**, *5* (3), 24-8.
5. Llor, C.; Bjerrum, L., Antimicrobial resistance: risk associated with antibiotic overuse and initiatives to reduce the problem. *Therapeutic advances in drug safety* **2014**, *5* (6), 229-241.
6. Davies, M. J.; Hawkins, C. L.; Pattison, D. I.; Rees, M. D., Mammalian heme peroxidases: from molecular mechanisms to health implications. *Antioxidants & redox signaling* **2008**, *10* (7), 1199-1234.
7. Kettle, A.; Winterbourn, C., Myeloperoxidase: a key regulator of neutrophil oxidant production. *Redox Report* **1997**, *3* (1), 3-15.
8. Ashby, M., Inorganic chemistry of defensive peroxidases in the human oral cavity. *Journal of dental research* **2008**, *87* (10), 900-914.
9. Bafort, F.; Damblon, C.; Smargiasso, N.; De Pauw, E.; Perraudin, J. P.; Jijakli, M. H., Reaction product variability and biological activity of the lactoperoxidase system depending on medium ionic strength and pH, and on substrate relative concentration. *Chemistry & biodiversity* **2018**, *15* (3), e1700497.

10. Ashby, M. T., Hypothiocyanite. In *Advances in Inorganic Chemistry*, Elsevier: **2012**; Vol. 64, pp 263-303.
11. Arlandson, M.; Decker, T.; Roongta, V. A.; Bonilla, L.; Mayo, K. H.; MacPherson, J. C.; Hazen, S. L.; Slungaard, A., Eosinophil peroxidase oxidation of thiocyanate characterization of major reaction products and a potential sulfhydryl-targeted cytotoxicity system. *Journal of Biological Chemistry* **2001**, 276 (1), 215-224.
12. Schlorke, D.; Flemmig, J.; Birkemeyer, C.; Arnhold, J., Formation of cyanogen iodide by lactoperoxidase. *Journal of inorganic biochemistry* **2016**, 154, 35-41.
13. Schlorke, D.; Atosuo, J.; Flemmig, J.; Lilius, E.-M.; Arnhold, J., Impact of cyanogen iodide in killing of *Escherichia coli* by the lactoperoxidase-hydrogen peroxide-(pseudo) halide system. *Free radical research* **2016**, 50 (12), 1287-1295.
14. Boening, D. W.; Chew, C. M., A critical review: general toxicity and environmental fate of three aqueous cyanide ions and associated ligands. *Water, air, and soil pollution* **1999**, 109 (1-4), 67-79.
15. Bak, B.; Hillebert, A., Cyanogen iodide- $\text{NaCN}^+ \text{I}_2^-$ $\text{ICN}^+ \text{NaI}$. *Organic Syntheses* **1952**, 32, 29-31.
16. Lunn, G.; Sansone, E. B., Destruction of cyanogen bromide and inorganic cyanides. *Analytical biochemistry* **1985**, 147 (1), 245-250.
17. Kumar, V., Cyanogen Bromide (CNBr). *Synlett* **2005**, 2005 (10), 1638-1639.
18. Shang, C.; Gong, W. L.; Blatchley, E. R., Breakpoint chemistry and volatile byproduct formation resulting from chlorination of model organic-N compounds. *Environmental Science & Technology* **2000**, 34 (9), 1721-1728.

19. West, M.; Lieu, T.; Krasner, S. In *Analytical determination of cyanogen bromide by electron-capture gas chromatography*, Proc. Am. Water Works Assoc. Water Qual. Technol. Conf., Orlando, FL, USA, **1991**.
20. Scilimenti, M.; Hwang, C.; Speitel, G.; Diehl, A. In *The simultaneous determination of cyanogen chloride and cyanogen bromide in chloraminated waters by a simplified microextraction GC/ECD technique*, Proc. 1994 AWWA Water Quality Technology Conf. Denver, CO: AWWA, **1995**.
21. Xie, Y.; Reckhow, D. A., A rapid and simple analytical method for cyanogen chloride and cyanogen bromide in drinking water. *Water Research* **1993**, 27 (3), 507-511.
22. Heller-Grossman, L.; Idin, A.; Limoni-Relis, B.; Rebhun, M., Formation of cyanogen bromide and other volatile DBPs in the disinfection of bromide-rich lake water. *Environmental science & technology* **1999**, 33 (6), 932-937.
23. Ohya, T.; Kanno, S., Formation of cyanide ion or cyanogen chloride through the cleavage of aromatic rings by nitrous acid or chlorine. X. Pathway of cyanogen chloride formation in the reactions of 1-naphthol and 4-phenylimidazole with chloramine. *Chemical and pharmaceutical bulletin* **1988**, 36 (10), 4095-4102.
24. Hirose, Y.; Maeda, N.; Ohya, T.; Nojima, K.; Kanno, S., Formation of cyanogen chloride by the reaction of amino acids with hypochlorous acid in the presence of ammonium ion. *Chemosphere* **1988**, 17 (5), 865-873.
25. Hirose, Y.; Maeda, N.; Ohya, T.; Nojima, K.; Kanno, S., Formation of cyanogen chloride by the reaction of peptides and proteins with hypochlorous acid in the presence of ammonium ion. *Chemosphere (Oxford)* **1989**, 18 (11-12), 2101-2108.

26. Ohya, T.; Kanno, S., Formation of cyanide ion or cyanogen chloride through the cleavage of aromatic rings by nitrous acid or chlorine. XI: On the reaction of purine bases with hypochlorous acid in the presence of ammonium ion. *Chemosphere* **1989**, *19* (12), 1835-1842.
27. Pedersen lii, E. J.; Mariñas, B. J., The hydroxide-assisted hydrolysis of cyanogen chloride in aqueous solution. *Water research* **2001**, *35* (3), 643-648.
28. Zgliczyński, J. M.; Stelmaszyńska, T., Hydrogen cyanide and cyanogen chloride formation by the myeloperoxidase-H₂O₂-Cl⁻ system. *Biochimica et Biophysica Acta (BBA)-Enzymology* **1979**, *567* (2), 309-314.
29. Schmidt, B.; Schröder, B.; Sonnenberg, K.; Steinhauer, S.; Riedel, S., From Polyhalides to Polypseudohalides: Chemistry Based on Cyanogen Bromide. *Angewandte Chemie International Edition* **2019**, *58* (30), 10340-10344.
30. Pedersen, E. J.; Urbansky, E. T.; Mariñas, B. J.; Margerum, D. W., Formation of cyanogen chloride from the reaction of monochloramine with formaldehyde. *Environmental science & technology* **1999**, *33* (23), 4239-4249.
31. Lei, H.; Minear, R. A.; Mariñas, B. J., Cyanogen bromide formation from the reactions of monobromamine and dibromamine with cyanide ion. *Environmental science & technology* **2006**, *40* (8), 2559-2564.
32. Gerritsen, C. M.; Gazda, M.; Margerum, D. W., Non-metal redox kinetics: hypobromite and hypoiodite reactions with cyanide and the hydrolysis of cyanogen halides. *Inorganic Chemistry* **1993**, *32* (25), 5739-5748.
33. Roberts, J. M.; Liu, Y., Solubility and solution-phase chemistry of isocyanic acid, methyl isocyanate, and cyanogen halides. *Atmospheric Chemistry & Physics* **2019**, *19* (7).

34. Hurrell, R. F., Bioavailability of iodine. *European journal of clinical nutrition* **1997**, *51*, S9-S12.
35. Zimmermann, M. B., Iodine deficiency. *Endocrine reviews* **2009**, *30* (4), 376-408.
36. Bowley, H. E.; Young, S. D.; Ander, E. L.; Crout, N.; Watts, M. J.; Bailey, E. H., Iodine binding to humic acid. *Chemosphere* **2016**, *157*, 208-214.
37. Hess, S. Y., The impact of common micronutrient deficiencies on iodine and thyroid metabolism: the evidence from human studies. *Best Practice & Research Clinical Endocrinology & Metabolism* **2010**, *24* (1), 117-132.
38. Winkler, R., Iodine—a potential antioxidant and the role of Iodine/Iodide in health and disease. *Natural Science* **2015**, *7* (12), 548.
39. Ahariz, M.; Courtois, P., Candida albicans susceptibility to lactoperoxidase-generated hypoiodite. *Clinical, cosmetic and investigational dentistry* **2010**, *2*, 69.
40. Xulu, B. A.; Ashby, M. T., Small molecular, macromolecular, and cellular chloramines react with thiocyanate to give the human defense factor hypothiocyanite. *Biochemistry* **2010**, *49* (9), 2068-2074.
41. Nagy, P.; Alguindigue, S. S.; Ashby, M. T., Lactoperoxidase-catalyzed oxidation of thiocyanate by hydrogen peroxide: a reinvestigation of hypothiocyanite by nuclear magnetic resonance and optical spectroscopy. *Biochemistry* **2006**, *45* (41), 12610-12616.
42. Lemma, K.; Ashby, M. T., Reactive sulfur species: Kinetics and mechanism of the reaction of hypothiocyanous acid with cyanide to give dicyanosulfide in aqueous solution. *Chemical research in toxicology* **2009**, *22* (9), 1622-1628.

43. Vona, R.; Gambardella, L.; Cittadini, C.; Straface, E.; Pietraforte, D., Biomarkers of oxidative stress in metabolic syndrome and associated diseases. *Oxidative medicine and cellular longevity* **2019**, 2019.
44. Tonoyan, L., Characterization of a novel antimicrobial agent inspired by. *Chem Res Toxicol* **2009**, 25 (2), 263-273.
45. Mandel, I.; Behrman, J.; Levy, R.; Weinstein, D., The salivary lactoperoxidase system in caries-resistant and-susceptible adults. *Journal of dental research* **1983**, 62 (8), 922-925.
46. Hawkins, C. L., The role of hypothiocyanous acid (HOSCN) in biological systems. *Free radical research* **2009**, 43 (12), 1147-1158.
47. Chandler, J. D.; Day, B. J., Thiocyanate: a potentially useful therapeutic agent with host defense and antioxidant properties. *Biochemical pharmacology* **2012**, 84 (11), 1381-1387.
48. Lemma, K.; Ashby, M. T., Reactive sulfur species: kinetics and mechanism of the equilibrium between cysteine sulfenyl thiocyanate and cysteine thiosulfinate ester in acidic aqueous solution. *The Journal of organic chemistry* **2008**, 73 (8), 3017-3023.
49. Ihalin, R.; Loimaranta, V.; Tenovu, J., Origin, structure, and biological activities of peroxidases in human saliva. *Archives of biochemistry and biophysics* **2006**, 445 (2), 261-268.
50. Nagy, P.; Lemma, K.; Ashby, M. T., Kinetics and mechanism of the comproportionation of hypothiocyanous acid and thiocyanate to give thiocyanogen in acidic aqueous solution. *Inorganic chemistry* **2007**, 46 (1), 285-292.
51. Conte, M. L.; Carroll, K. S., The chemistry of thiol oxidation and detection. In *Oxidative stress and redox regulation*, Springer: **2013**; pp 1-42.

52. Derscheid, R. J.; van Geelen, A.; Berkebile, A. R.; Gallup, J. M.; Hostetter, S. J.; Banfi, B.; McCray Jr, P. B.; Ackermann, M. R., Increased concentration of iodide in airway secretions is associated with reduced respiratory syncytial virus disease severity. *American journal of respiratory cell and molecular biology* **2014**, *50* (2), 389-397.
53. Nagy, P.; Jameson, G. N.; Winterbourn, C. C., Kinetics and mechanisms of the reaction of hypothiocyanous acid with 5-thio-2-nitrobenzoic acid and reduced glutathione. *Chemical research in toxicology* **2009**, *22* (11), 1833-1840.
54. Albrich, J. M.; McCarthy, C. A.; Hurst, J. K., Biological reactivity of hypochlorous acid: implications for microbicidal mechanisms of leukocyte myeloperoxidase. *Proceedings of the National Academy of Sciences* **1981**, *78* (1), 210-214.
55. Rosen, H.; Klebanoff, S., Oxidation of Escherichia coli iron centers by the myeloperoxidase-mediated microbicidal system. *Journal of Biological Chemistry* **1982**, *257* (22), 13731-13735.
56. Schraufstatter, I.; Browne, K.; Harris, A.; Hyslop, P. A.; Jackson, J. H.; Quehenberger, O.; Cochrane, C., Mechanisms of hypochlorite injury of target cells. *The Journal of clinical investigation* **1990**, *85* (2), 554-562.
57. Woods, A. A.; Davies, M. J., Fragmentation of extracellular matrix by hypochlorous acid. *Biochemical Journal* **2003**, *376* (1), 219-227.
58. Nagy, P.; Ashby, M. T., Reactive sulfur species: kinetics and mechanisms of the oxidation of cysteine by hypohalous acid to give cysteine sulfenic acid. *Journal of the American Chemical Society* **2007**, *129* (45), 14082-14091.

59. Skaff, O.; Pattison, D. I.; Davies, M. J., Hypothiocyanous acid reactivity with low-molecular-mass and protein thiols: absolute rate constants and assessment of biological relevance. *Biochemical Journal* **2009**, *422* (1), 111-117.
60. Lloyd, M. M.; van Reyk, D. M.; Davies, M. J.; Hawkins, C. L., Hypothiocyanous acid is a more potent inducer of apoptosis and protein thiol depletion in murine macrophage cells than hypochlorous acid or hypobromous acid. *Biochemical Journal* **2008**, *414* (2), 271-280.
61. Winterbourn, C. C.; Metodiewa, D., Reactivity of biologically important thiol compounds with superoxide and hydrogen peroxide. *Free Radical Biology and Medicine* **1999**, *27* (3-4), 322-328.
62. Ihalin, R.; Nuutila, J.; Loimaranta, V.; Lenander, M.; Tenovuo, J.; Lilius, E.-M., Susceptibility of *Fusobacterium nucleatum* to killing by peroxidase–iodide–hydrogen peroxide combination in buffer solution and in human whole saliva. *Anaerobe* **2003**, *9* (1), 23-30.
63. Bosch, E. v.; Van Doorne, H.; De Vries, S., The lactoperoxidase system: the influence of iodide and the chemical and antimicrobial stability over the period of about 18 months. *Journal of applied Microbiology* **2000**, *89* (2), 215-224.
64. Wei, Y. J.; Liu, C. G.; Mo, L. P., Ultraviolet absorption spectra of iodine, iodide ion and triiodide ion. *Guang pu xue yu guang pu fen xi= Guang pu* **2005**, *25* (1), 86.
65. McGowan Jr, J. E., Economic impact of antimicrobial resistance. *Emerging infectious diseases* **2001**, *7* (2), 286.
66. Amenu, D., Antimicrobial activity of medicinal plant extracts and their synergistic effect on some selected pathogens. *American Journal of Ethnomedicine* **2014**, *1* (1), 18-29.

67. Slungaard, A.; Mahoney, J. R., Thiocyanate is the major substrate for eosinophil peroxidase in physiologic fluids. Implications for cytotoxicity. *Journal of Biological Chemistry* **1991**, 266 (8), 4903-4910.
68. Pruitt, K.; Tenovuo, J., The lactoperoxidase system: chemistry and biological significance. immunology series. Vol. 27. **1985**. Marcel Dekker: New York.

Chapter 2

2. Experimental Procedures

2.1. Reagents and Buffer Solutions

All chemicals were purchased from Sigma Aldrich. Lactoperoxidase from bovine milk, iodine (I_2 , 99.8%), potassium iodide (KI, 99.5%), hydrogen peroxide (H_2O_2 , 30 wt.% in H_2O), potassium thiocyanate, (KSCN, 99%), sodium phosphate monobasic dihydrate ($NaH_2PO_4 \cdot 2H_2O$, 99%), and sodium phosphate dibasic (Na_2HPO_4 , 99%), sodium hydroxide (NaOH, 98%), sodium hypochlorite (NaOCl, 98%) sodium chloride (NaCl, %), hydrochloric acid (HCl, 32%), sodium cyanide (NaCN, 97%), diethyl ether ($(CH_3CH_2)_2O$, 99.7%), potassium thiocyanate-13-C ($KS^{13}CN$, 99%) and 15-N ($KSC^{15}N$, 99%), 5,5'-dithiobis-(2-nitrobenzoic acid) (DTNB, 98%), β -mercaptoethanol (99%), glutathione (GSH, 98%), cysteamine ($NH_2CH_2CH_2SH$, 95%), penicillamine ($(CH_3)_2C(SH)CH(NH_2)CO_2H$, 99%), L-cysteine (Cys, 98%), L-cysteine ($HSCH_2CH(NHCOCH_3)CO_2H$, 99%), bovine serum albumin-thiols containing protein (BSA, 96%) were used as received from Sigma Aldrich. Water used for all aqueous solutions was doubly-distilled in glass.

The 0.1 M phosphate buffer (pH 7.4) solution was prepared by dissolving accurately weighed quantities of $NaH_2PO_4 \cdot 2H_2O$ and Na_2HPO_4 in 1 L volumetric flask which was filled to the mark with distilled water. The ionic strength was adjusted with $NaClO_4$ and the pH adjustments were made with dilute HCl and NaOH as necessary. A 0.5 M Tris-HCl buffer (pH 8.8) was prepared by dissolving 32.285 g of Tris in a 1 L volumetric flask and filled to the mark with distilled water and pH adjusted accordingly using HCl.

Fresh aqueous solutions of OSCN^- were prepared enzymatically using LPO-catalyzed oxidation of SCN^- with H_2O_2 . LPO ($\sim 0.1 \mu\text{M}$) was incubated with SCN^- (5 mM) and the reaction was initiated by the addition of H_2O_2 (1 mM) in 0.1 M phosphate buffer (pH 7.4) at room temperature. The concentration of OSCN^- stock solution was quantified by absorbance at $\epsilon_{376\text{nm}} = 25.6 \text{ M}^{-1} \text{ cm}^{-1}$.¹ OSCN^- solution was used within 1 hr of preparation due to its low stability. This method typically produced $\sim 1 \text{ mM}$ OSCN^- . UV-vis spectra were collected using an Ocean Optics UBC2000 CCD spectrometer equipped with a 1 meter WPI fiber optic cell and an ATS D 1000 CE UV light source.

2.1.1. Iodine preparation

Aqueous iodine solution was prepared using reagent grade iodine (I_2) granules. Due to partial solubility of I_2 in distilled water, granulated I_2 was stirred in distilled water for about 24 hours.² To prevent the oxidation of the aqueous solution by light, containers were kept covered with the aluminium foil for the duration of the shaking. The concentration of I_2 was determined spectroscopically using UV-Vis ($\lambda_{\text{max}} = 203 \text{ nm}$, $\epsilon = 19\,600 \text{ M}^{-1} \text{ cm}^{-1}$).³

2.1.2. Synthesis of cyanogen iodide (ICN)

The method used was adopted with few modification from Bak and Hillebert.⁴ In a three-necked 500 mL flask with a thermometer, sodium cyanide (NaCN) (27 g, 0.55 mole) was dissolved in 100 mL of distilled water and cooled to 4 °C. Iodine (I_2) (127 g) was added while stirring in portions of about 3 to 4 g every 5 minutes over a period of approximately 30 minutes. After ten minutes of I_2 addition, cold diethyl ether (120 mL)

was added. The reaction mixture was stirred for a few minutes until all the precipitate was completely dissolved. The organic layer and the aqueous layer were separated with a previously cooled separating funnel. The organic layer was evaporated under reduced pressure at room temperature and in the dark. The entire contents were vigorously stirred at 50 °C for 15 minutes. The mixture was then cooled to 0 °C and the slightly yellow crystalline cyanogen iodide was filtered and rinsed off with six 25 mL portions of cold water. For highest purity of cyanogen iodide, the obtained product was dissolved in 150 mL of boiling chloroform and filtered on a hot-water funnel. The solution was cooled at room temperature for 15 minutes, followed by ice cooling to 0 °C. It was filtered by means of suction and washed with 15 mL of cold chloroform three times. Traces of solvents were further evaporated at room temperature in a fume hood. ICN crystals were characterized by the UV-Vis spectroscopy at its maximum absorbance 222 nm. The molar extinction coefficient of ICN was determined to be 179 M⁻¹ s⁻¹. The authenticity of ICN was further confirmed by ¹³C NMR spectroscopy, mass spectrometry, Raman spectroscopy and FT-IR spectroscopy.

2.2. Instrumentation

2.2.1. UV-Vis spectroscopy

Most of the spectrophotometric was carried out with a Cary 100 UV-visible spectrophotometer from Agilent technology in a 1 cm path length quartz cell. An ocean optic recording instrument equipped with a 1 meter fibre optic cell was employed for the determination of OSCN⁻ concentration ($\lambda_{\text{max}} = 376 \text{ nm}$, $\epsilon = 26.5 \text{ M}^{-1} \text{ cm}^{-1}$).

2.2.2. pH Measurements

The pH measurements of the buffered solutions were performed with a Metrohm 827 pH meter. The pH-meter was calibrated with standard pH reagents. The ionic strength was kept constant at 1.0 M for most solutions using NaClO.

2.2.3. Stopped-flow studies

Stopped-flow experiments were carried out using the single-mixing mode. Polychromatic data was obtained from the stopped-flow analyser (Applied photophysics, SX20) equipped with a Xenon arch lamp and a photodiode detector, covering the spectral range of 190–730 nm. Pro-Data viewer software was used to process the kinetic data, *SPECFIT* (version 3.0.40) was used to deconvolute polychromatic data and to perform kinetic simulations. Kinetic plots were prepared with OriginPro (version 9.1) software.

2.2.4. Mass Spectrometry

Mass spectrometry experiments were carried out on a Water Micromass LCT premier MS instrument equipped with electrospray ionization (ESI) source and time-of-flight (TOF) mass analyser. The instrument was operated in a positive ion mode. Samples were injected directly into the instrument. Mass spectra were recorded in the 100-1000 m/z range.

2.2.5. ¹³C NMR Measurements

¹³C NMR spectra were recorded with a Bruker 500 MHz NMR spectrometer. All measurements were performed using standard NMR tubes at 30 °C. Deuterium oxide (10% D₂O) was employed as a frequency lock. Data was analysed using Topspin 2.1, a Bruker software.

2.2.6. Infrared (IR) Spectroscopy

In this spectroscopic technique, aqueous solutions were placed on an Art Diamond-1 bounce sample holder, followed by immediate collection of the spectrum. A Cary 100 FT-IR spectrometer from Agilent technology was used. The FT-IR data was processed with OriginPro (version 9.1) software.

2.3. Competition kinetic studies

Second-order rate constants for the reactions of TNB with ICN were measured under pseudo-first-order conditions by stopped-flow technique. The kinetic experiments were conducted with at least a 10-fold excess of TNB over ICN. The reaction was monitored using the diode-array on the stopped-flow instrument in a single-mixing mode at 412 nm. Rate constants for the reactions of free and protein thiols were determined by competition with TNB for ICN. Competition experiments involved premixing TNB with the other thiol and then reacting the mixture with an equal volume of ICN. ICN was kept a limiting reagent and the reaction was monitored by following the loss of TNB at 412 nm.

2.4. Antimicrobial studies

The antimicrobial activity of ICN solutions (5 – 50 μM) against *Escherichia coli* ATCC 25922 strains was determined according to the European Committee on Antimicrobial Susceptibility Testing (EUCAST) criteria. Briefly, the bacterial strains were cultured and incubated for 24 h at 37 °C in a nutrient agar broth until an optical density of 0.15 to 0.30 (620 nm) was obtained. Glycerol stock of the *E. coli* cell cultures were spotted on agar plates and following treatment, the agar plates were kept in dark conditions at room temperature for 30 days. The parts of the agar plate where there was no longer bacterial growth (growth inhibition) were indicative of the minimum inhibitory concentration (MIC). All experiments were done in duplicate, and we will include controls with selected reference biocides such as formaldehyde.

2.5. Reference

1. Nagy, P.; Alguindigue, S. S.; Ashby, M. T., Lactoperoxidase-catalyzed oxidation of thiocyanate by hydrogen peroxide: a reinvestigation of hypothiocyanite by nuclear magnetic resonance and optical spectroscopy. *Biochemistry* **2006**, *45* (41), 12610-12616.
2. Simoyi, R. H.; Epstein, I. R.; Kustin, K., Systematic design of chemical oscillators. 49. Kinetics and mechanism of the autoinhibitory iodine-thiocyanate reaction. *The Journal of Physical Chemistry* **1989**, *93* (7), 2792-2795.
3. Wei, Y. J.; Liu, C. G.; Mo, L. P., Ultraviolet absorption spectra of iodine, iodide ion and triiodide ion. *Guang pu xue yu guang pu fen xi= Guang pu* **2005**, *25* (1), 86-88.
4. Bak, B.; Hillebert, A., Cyanogen Iodide- $\text{NaCN}^+ \text{I}_2^-$] $\text{ICN}^+ \text{NaI}$. *Organic Syntheses* **1952**, *32*, 29-31.
5. Miron, T.; Rabinkov, A.; Mirelman, D.; Weiner, L.; Wilchek, M., A spectrophotometric assay for allicin and alliinase (Alliin lyase) activity: reaction of 2-nitro-5-thiobenzoate with thiosulfinates. *Analytical biochemistry* **1998**, *265* (2), 317-325.

Chapter 3

3. Results and Discussion

3.1. Production of ICN via a non-enzyme system

3.1.1. Reaction of I⁻ with OSCN⁻ to form I₂

Researchers generally agree that in the oral cavity, OSCN⁻ is the main product of primary peroxidase enzymes. A series of chemical reactions involving iodide occur following the production of hypohalites. These non-enzymatic pathways produce iodine-based antimicrobial species. Paquette *et al*, have reported that HOCl can oxidize I⁻ to OI⁻/HOI depending upon the pH. HOI is formed in acidic media and OI⁻ is formed in basic conditions. Excess iodide (I⁻) further reacts with IO⁻/HOI to form I₂ as shown in reaction 8 and 9.



Figure 1 shows spectra obtained shortly after mixing OSCN⁻ with I⁻ as a function of time. The absorption spectra are very similar to those previously reported for HOI/OI⁻ in chemical literature.¹ The spectrum features absorption bands mainly at 376 and ~250 nm for OSCN⁻, and a shoulder around 425 nm that is attributed to lactoperoxidase (LPO). Ashby *et al* cautioned against recording the OSCN⁻ spectrum below 300 nm due to domination by other more absorbing species including thiocyanate and lactoperoxidase. They further indicated that the absorption at 376 nm is the more characteristic feature of OSCN⁻ despite the low molar extinction coefficient of 26.5 M⁻¹

1 cm^{-1} at this wavelength. In the region between the two isosbestic points at 280 nm and 350 nm, the growing absorption band is consistent with the presence of HOI. The HOI band previously observed $\sim 278 \text{ nm}$ at pH 12 has shifted to $\sim 303 \text{ nm}$ at pH 7.4. The insert shows the rate at which OSCN^- is reacting with I^- under the conditions of our experiments in the presence of lactoperoxidase.

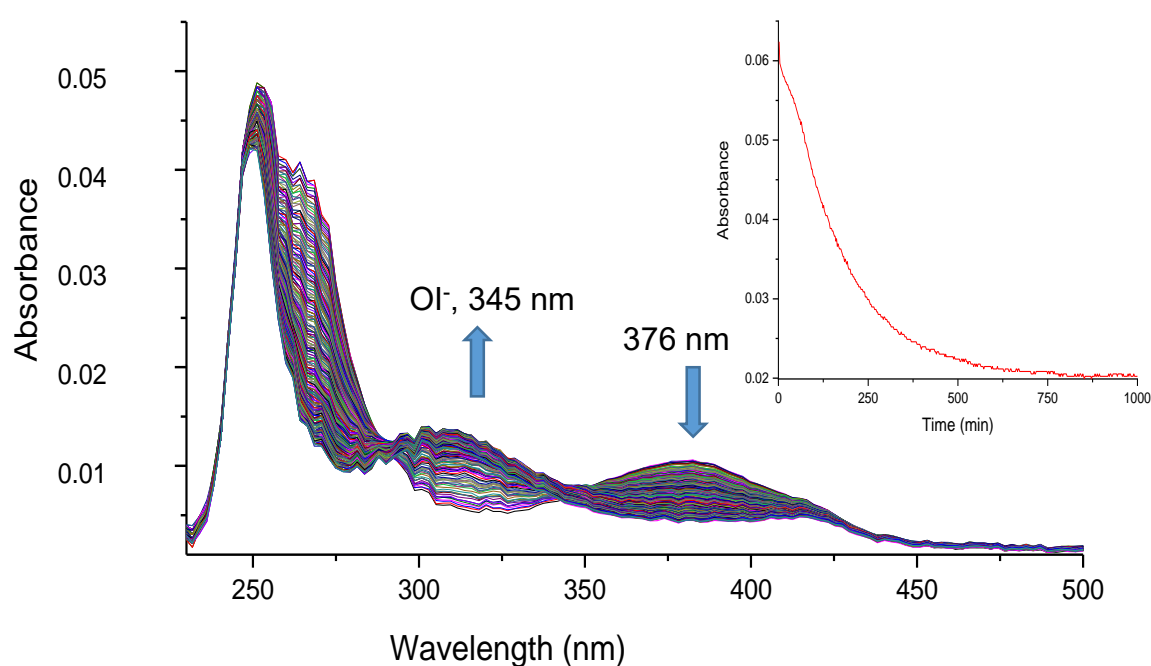


Figure 1: Time resolved spectra showing the formation of hypoiodite ion (OI^-) and the disappearance of OSCN^- .

The time course for the formation and disappearance of HOI was determined by monitoring changes in the maximum absorption between 280-350 nm. The formation

of HOI occurs between 0 to 490 minutes after which, its decomposition commences as it reacts with excess I^- to yield I_2 as the final stable product.

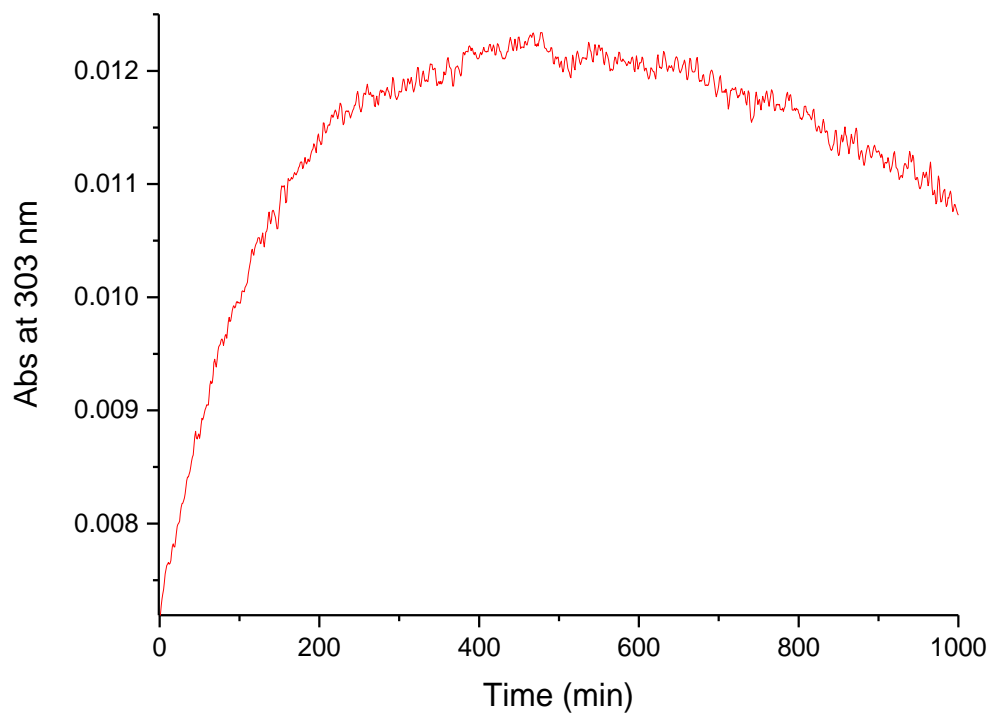


Figure 2: Kinetic trace for the formation and decomposition of HOI between 280-345 nm.

3.1.2. Reaction of I₂ with SCN⁻ to produce cyanogen iodide (ICN)

The changes in the UV spectra occurring when I₂ is reacted with SCN⁻ are shown in Figure 3. Cyanogen iodide the product formed by this reaction has an absorbance band at 222 nm. Other prominent spectral features are the isosbestic point at 218 nm and a band at 203 nm due to the disappearance of I₂.² The reaction is pH sensitive, being faster in phosphate buffered solutions at pH 7.4 than in unbuffered solutions. In distilled water, the reaction pH drops rapidly to about pH 6.3 after the reaction.

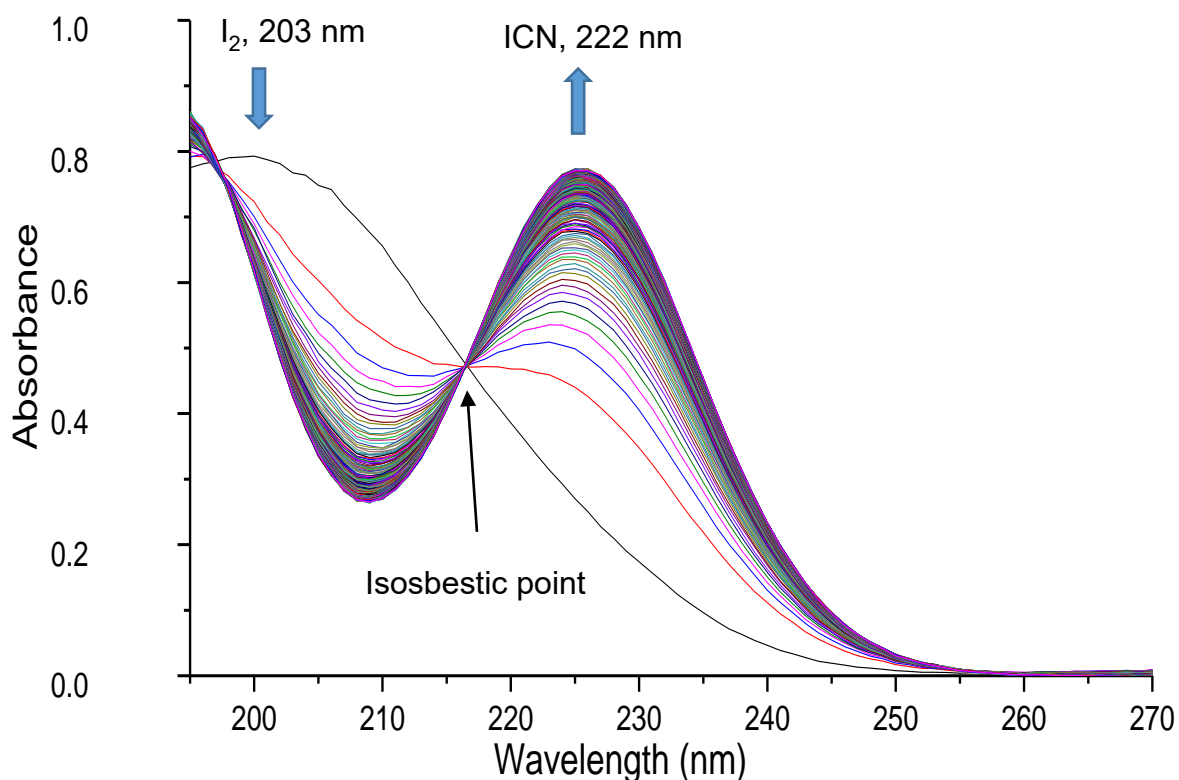


Figure 3: Time resolved spectral changes showing the formation of ICN in distilled water.

The time course of ICN formation was monitored through spectral changes at 222 nm. The kinetic trace indicates a slow reaction (minute-time scale) and high ICN stability at pH 7.4 as shown in Figure 4.

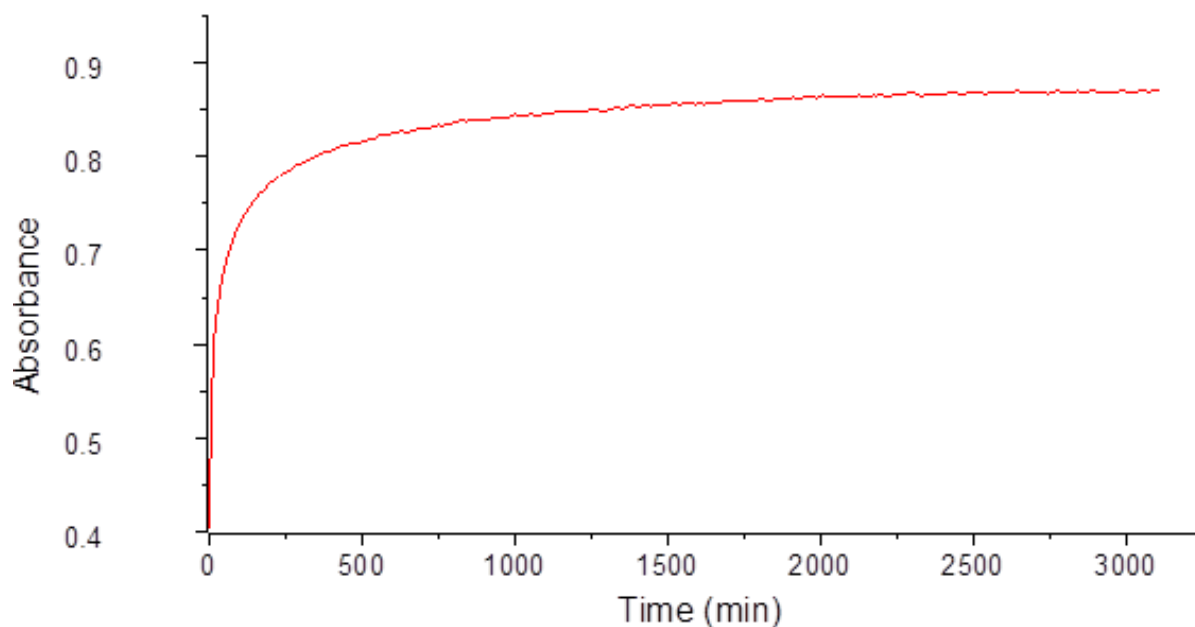


Figure 4: Kinetic trace showing the formation of ICN at 222 nm over time.

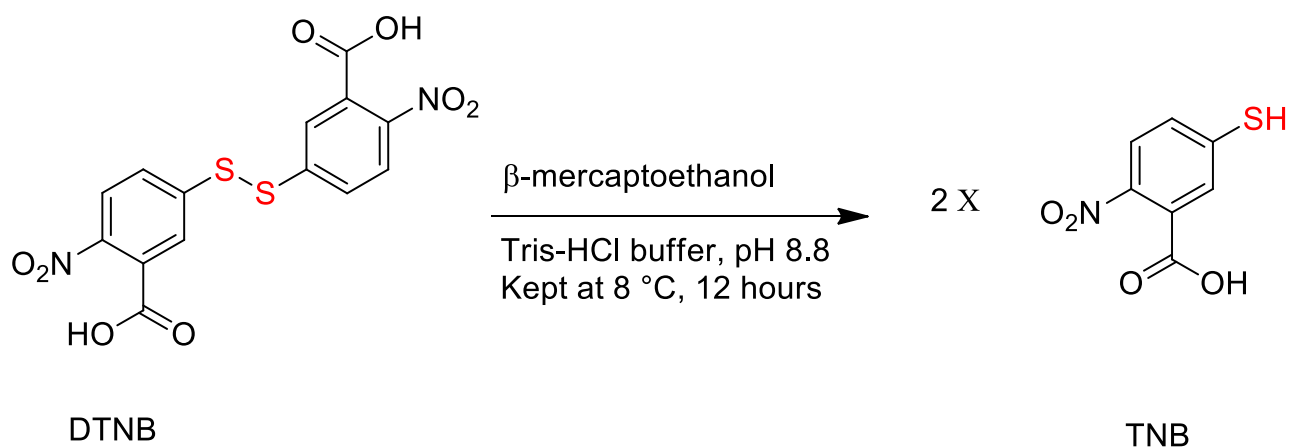
The formation of ICN under the conditions of our experiments was further confirmed using ^{13}C -labelled SCN^- . The nature of the ^{13}C -labelled oxidation product was studied using ^{13}C NMR spectroscopy. The reaction of ^{13}C -labelled thiocyanate (S^{13}CN , 133.4 ppm) with I_2 produced a signal with a chemical shift at 49.8 ppm as shown in Figure 5. In the chemical literature, the chemical shift data reported for the ICN signal is reported between 51-53 ppm for enzyme catalysed reactions, 49.5 ppm for commercial pure product in distilled water (pH 4 and 7) ³ and 51.1–51.8 ppm for ICN in buffered I^- solution. ⁴⁻⁵



Figure 5: ^{13}C NMR spectra for the reaction of I_2 with S^{13}CN in deionized water.

3.2. Synthesis of 5-thio-2-nitrobenzoic acid (TNB)

TNB was obtained as orange crystals from the reduction of the Ellman's reagent 5,5'-dithiobis-2-nitrobenzoic acid (DTNB) by β -mercaptoethanol as shown in Scheme 2.



Scheme 1: Formation of TNB from the reduction of DTNB.

The purity of TNB was confirmed by UV-Vis spectroscopy at its maximum absorption of 412 nm (Figure 6).

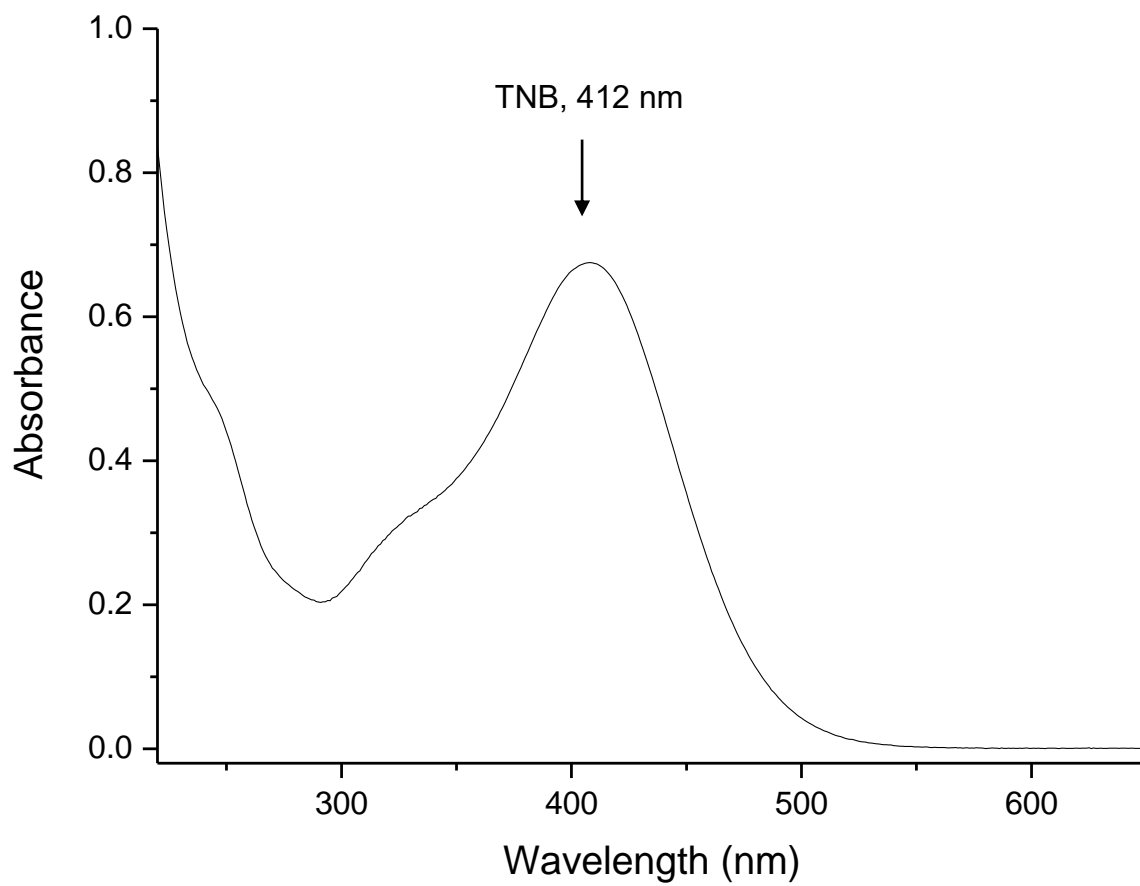
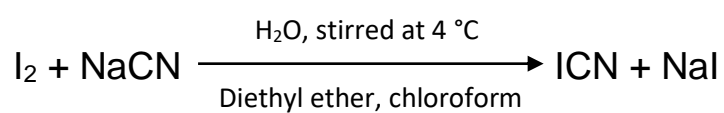


Figure 6: The UV-Vis spectra of TNB in phosphate buffer at pH 7.4.

3.3. Synthesis of cyanogen iodide (ICN)

Cyanogen iodide was successfully synthesized as white needle like crystals by the sublimation of iodine and sodium cyanide.⁶ The formation and authenticity of ICN was confirmed by UV-Vis spectroscopy, nuclear magnetic resonance (NMR), infra-red (IR) and Raman spectroscopy.



Scheme 2: Synthetic pathway for ICN.

3.4. Characterization of cyanogen iodide (ICN)

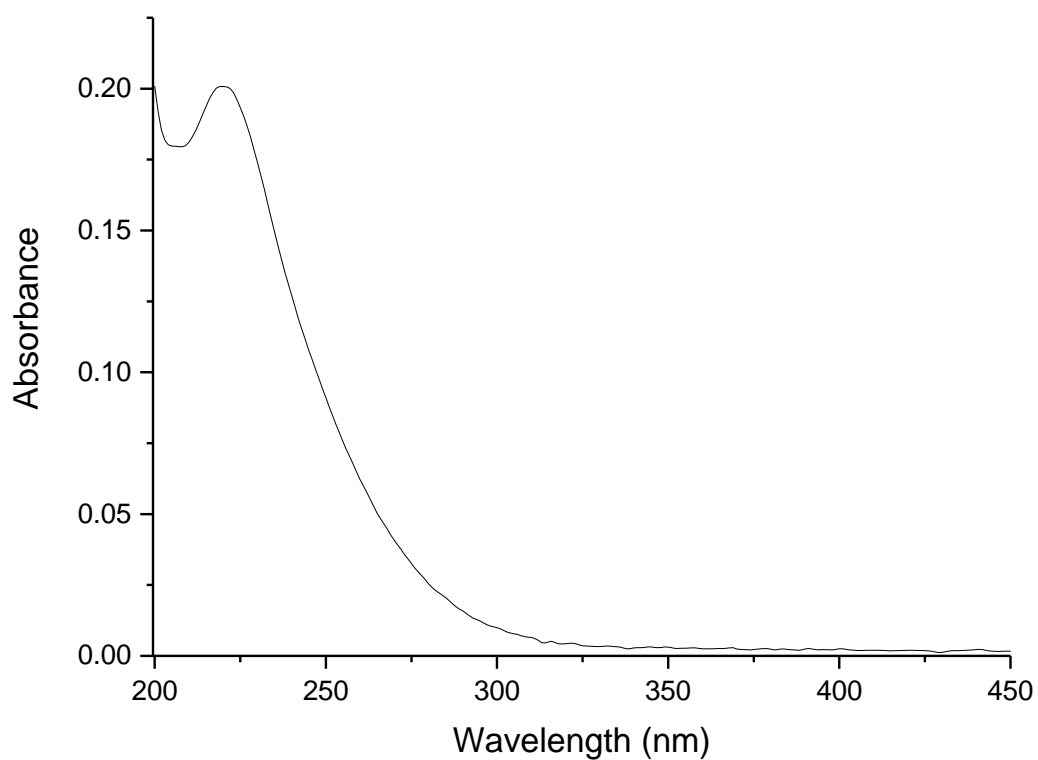


Figure 7: The UV-Vis spectrum of ICN, maximum absorption at 222 nm, $\epsilon = 179 \text{ M}^{-1} \text{ cm}^{-1}$.

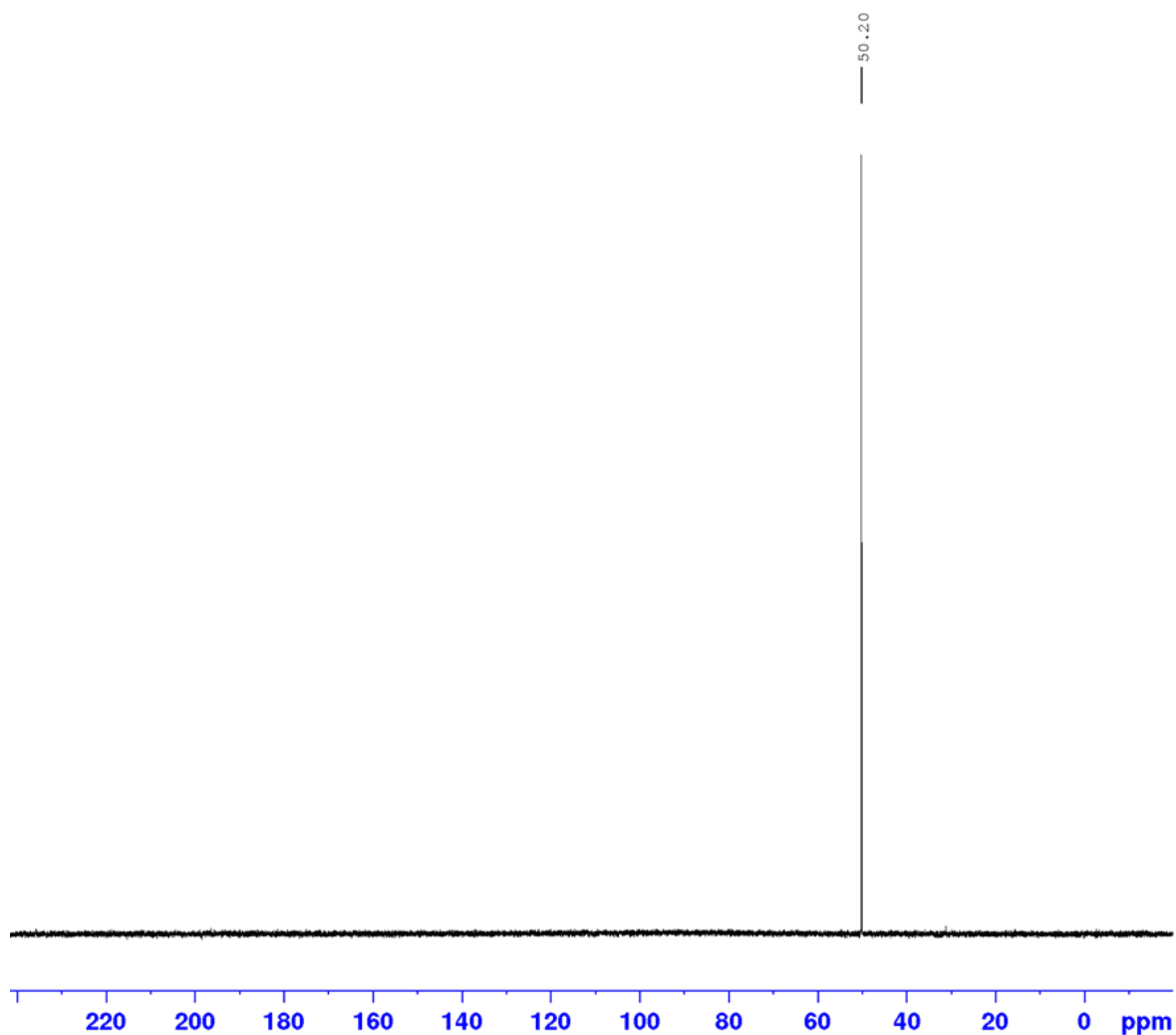


Figure 8: ¹³C NMR spectrum of ICN.

Cyanogen iodide (ICN) was identified by its chemical shift at 50.20 ppm, a value that correlates well with literature data reported by Schlorke *et al* for pure ICN, which showed a signal at 50.1 ppm. In addition to ICN, Schlorke also reported the formation of a new singlet signal with a chemical shift approximately 53.0 ppm upon further addition of I⁻ suggesting the presence of I₂CN⁻.⁴

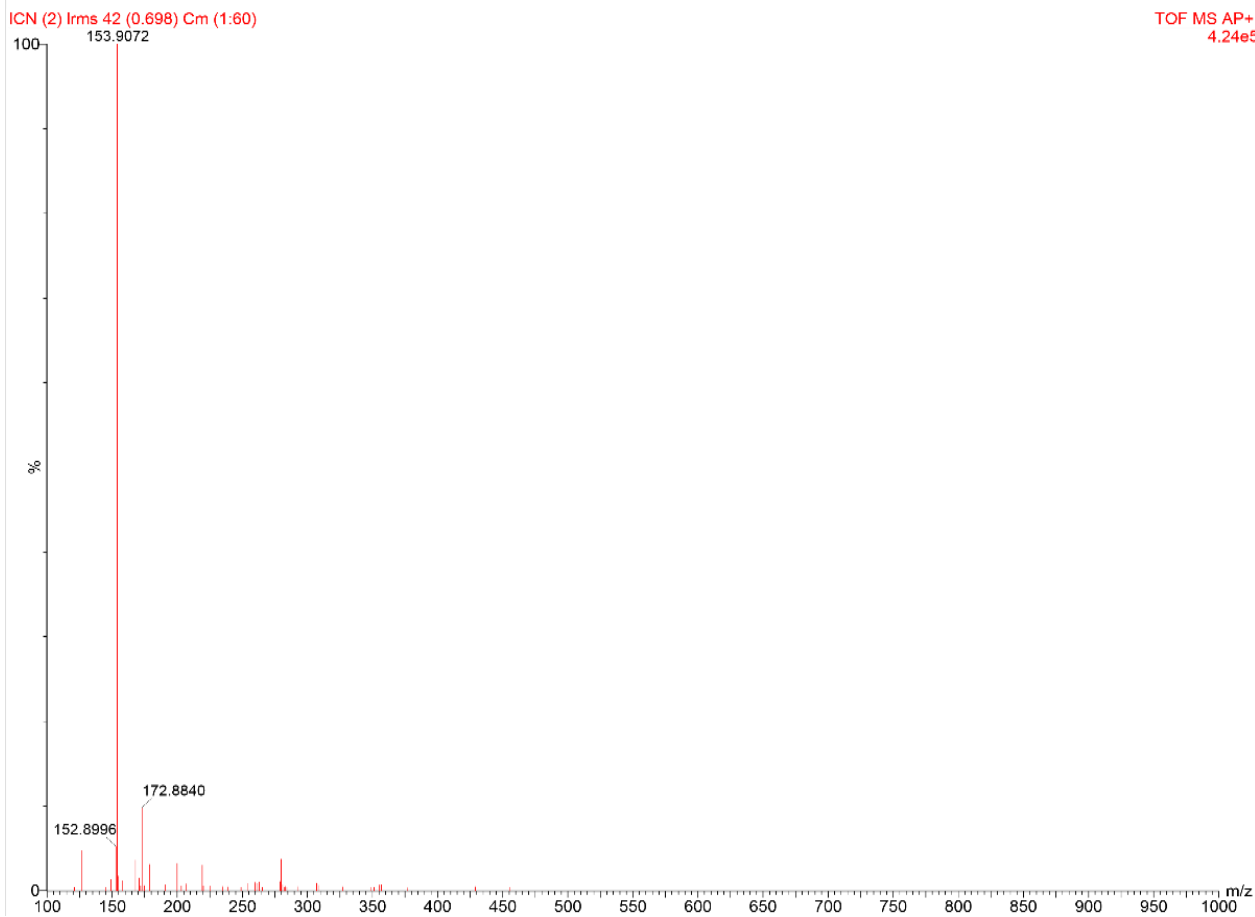


Figure 9: Mass spectrum of ICN in the positive ion mode.

The mass spectrum of ICN (Figure 9) obtained from the TOF-MS showed a base peak in the positive ion mode $[M+1]$, $m/z = 153.9072$. This peak confirms the formation of ICN which has a molecular mass of $152.92 \text{ g}\cdot\text{mol}^{-1}$.

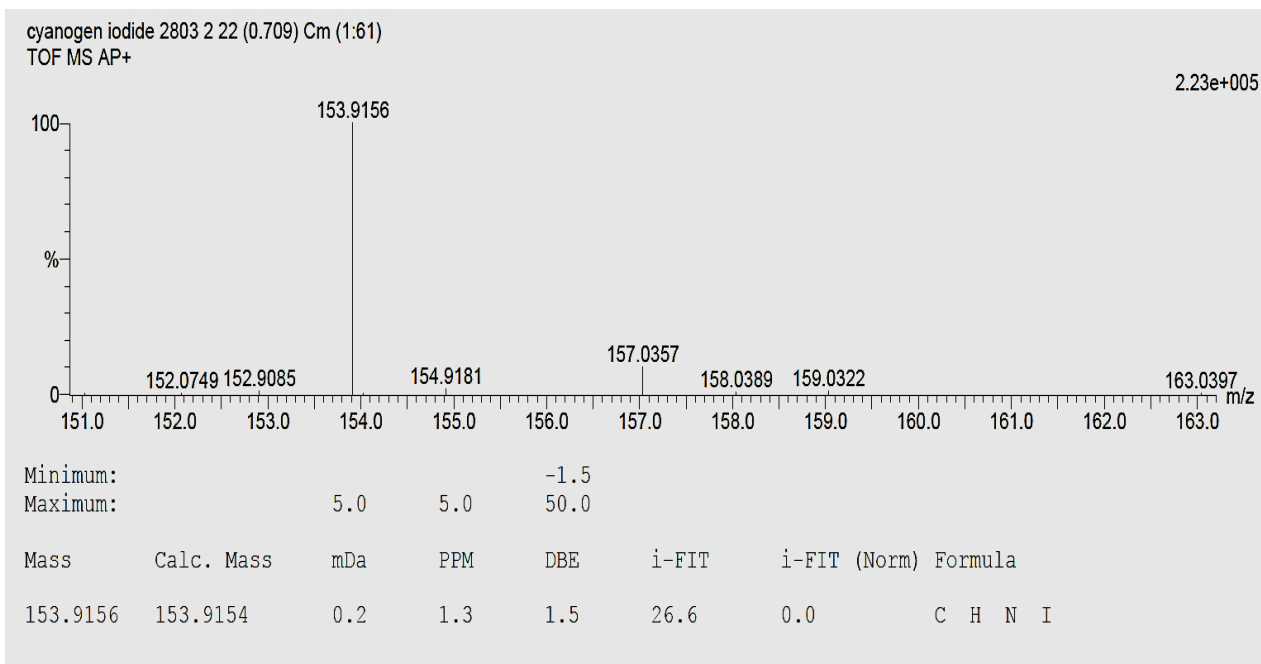


Figure 10: Accurate mass spectrum of ICN in the positive ion mode.

The mass spectrum of ICN in Figure 10 showed a peak of interest in the positive ion mode [M+1], $m/z = 153.9156$. This confirms the authenticity of ICN.

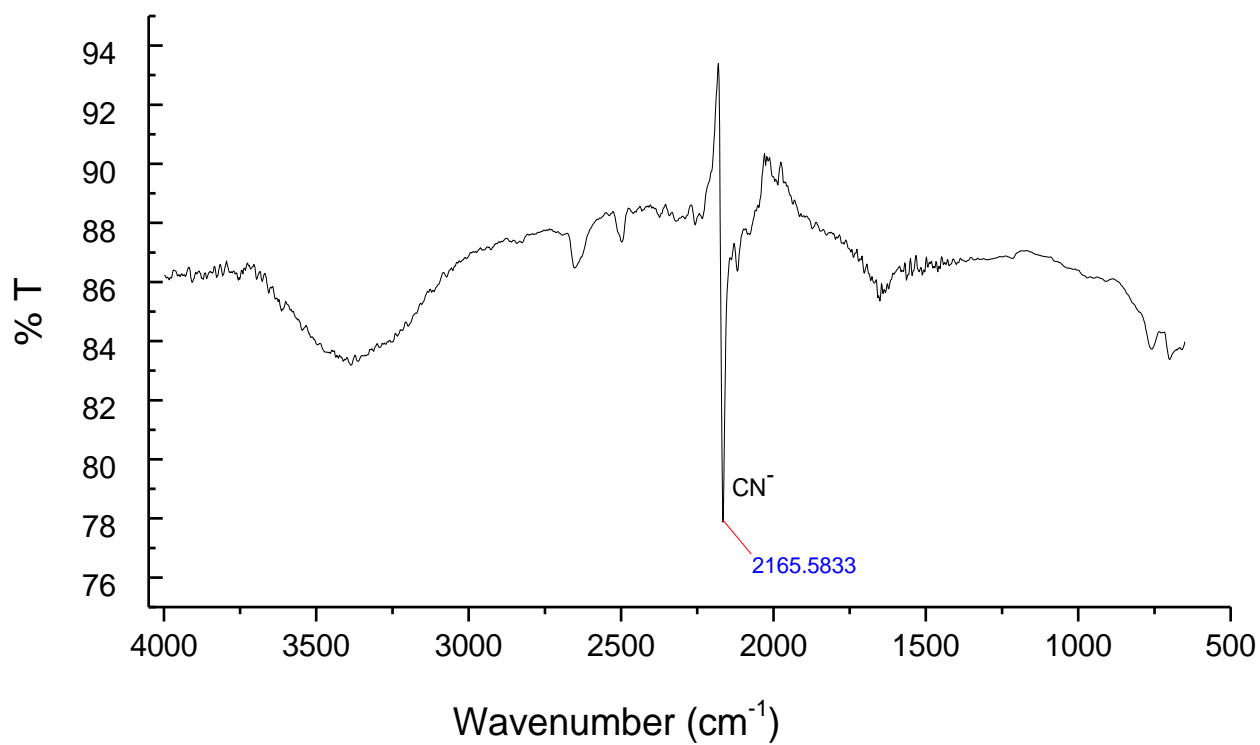


Figure 11: FT-IR spectrum of ICN.

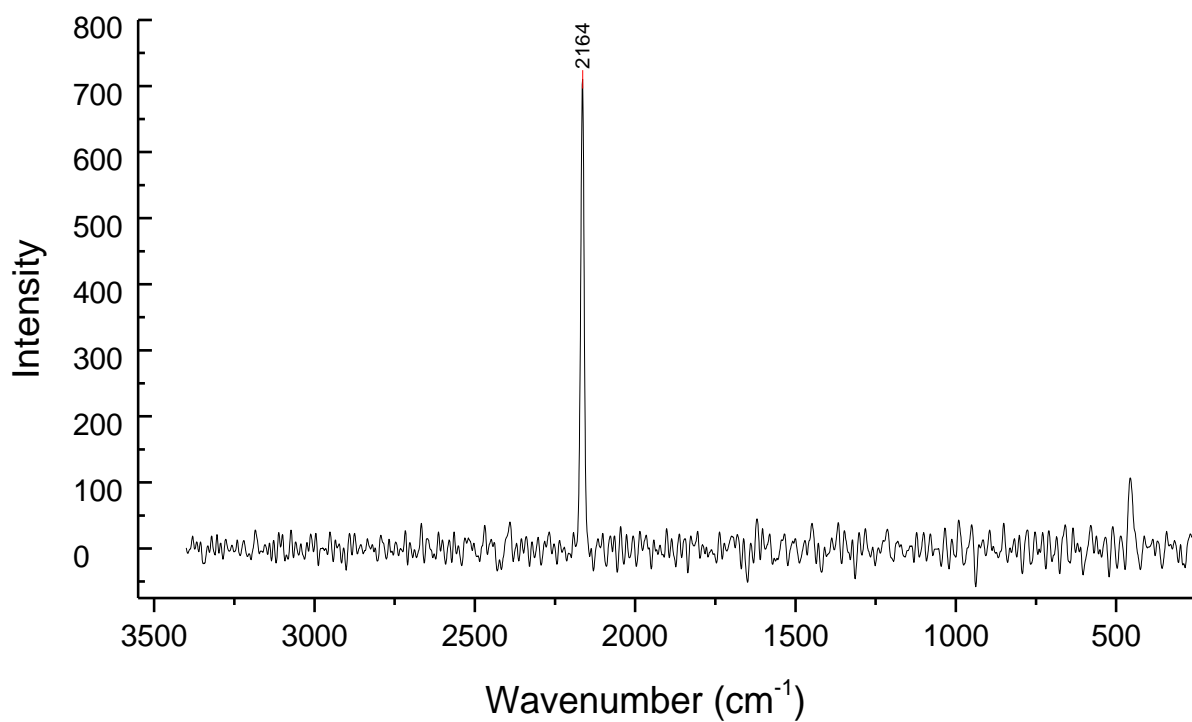


Figure 12: Raman spectrum of ICN.

The presence of the intense CN stretch at 2165.6 cm⁻¹ in the infrared spectrum combined with the Raman spectrum showing a band at 2164 cm⁻¹ confirms the presence of ICN. These IR data are in agreement with those reported by Chadwick *et al.*⁷

3.5. Oxidation of selected biological thiols by ICN

3.5.1. Reaction of ICN with TNB

The rate constant for the reaction of ICN with TNB was measured directly by the stopped-flow technique. The second-order rate constant obtained for the reaction of TNB was later used as a reference in subsequent competition kinetic experiments involving other biological thiol groups. The reaction was studied by following the disappearance of TNB maximum absorbance at 412 nm. The polychromatic data featured in Figure 13 is characterized by simultaneous disappearance of TNB at 412 nm and DTNB formation at 324 nm, which are separated by a clear isosbestic point at approximately 362 nm. In all the stopped-flow experiments, pseudo-first-order conditions were employed using excess TNB over ICN.

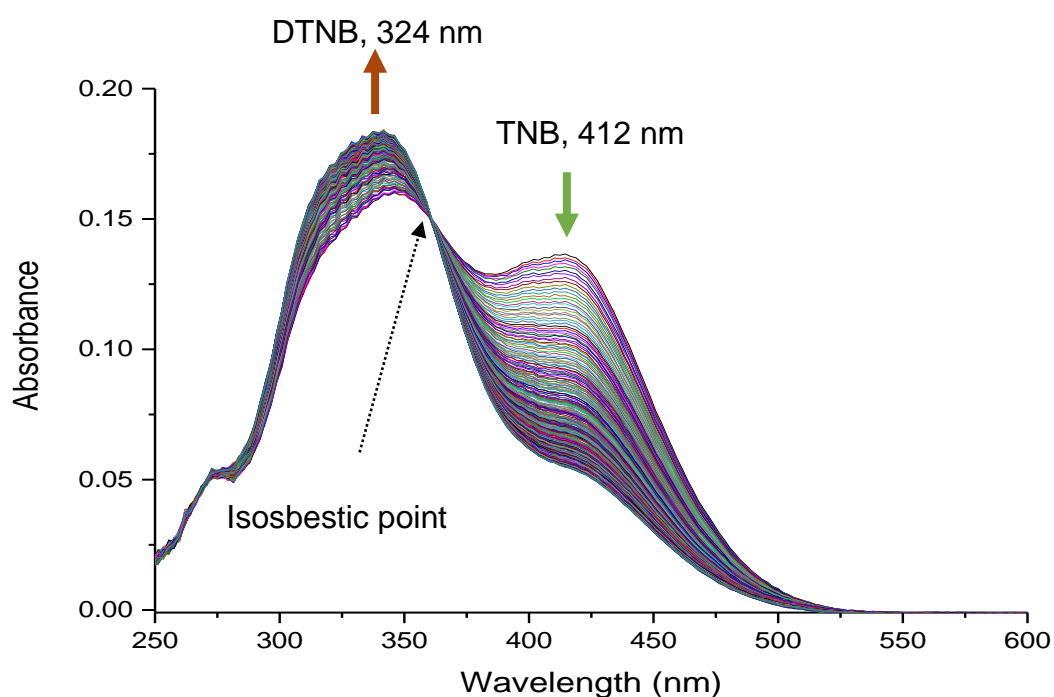


Figure 13: Time-resolved spectral changes observed after reacting ICN (10 μM) with TNB (50 μM).

The rate constant for reaction of the ICN (10 μM) with TNB (50-250 μM) was determined by fitting kinetic data obtained at 412 nm to a single exponential function. The fitting of kinetic traces at 412 nm resulted in the observed rate constants (k_{obs}). When k_{obs} values were plotted against TNB concentration, it showed a linear dependence that demonstrates that the reaction is first order in [TNB] (Figure 15, see Figure 20 in appendix 1 for typical linear plot). The gradient of the linear plot yielded a second-order rate constant of $2.1 \times 10^4 \text{ M}^{-1} \text{ s}^{-1}$. To simulate the acidic conditions in the phagosome⁸⁻¹⁰, the rate constant for the reaction of TNB with ICN was also determined at pH 6.0 (Table 2).

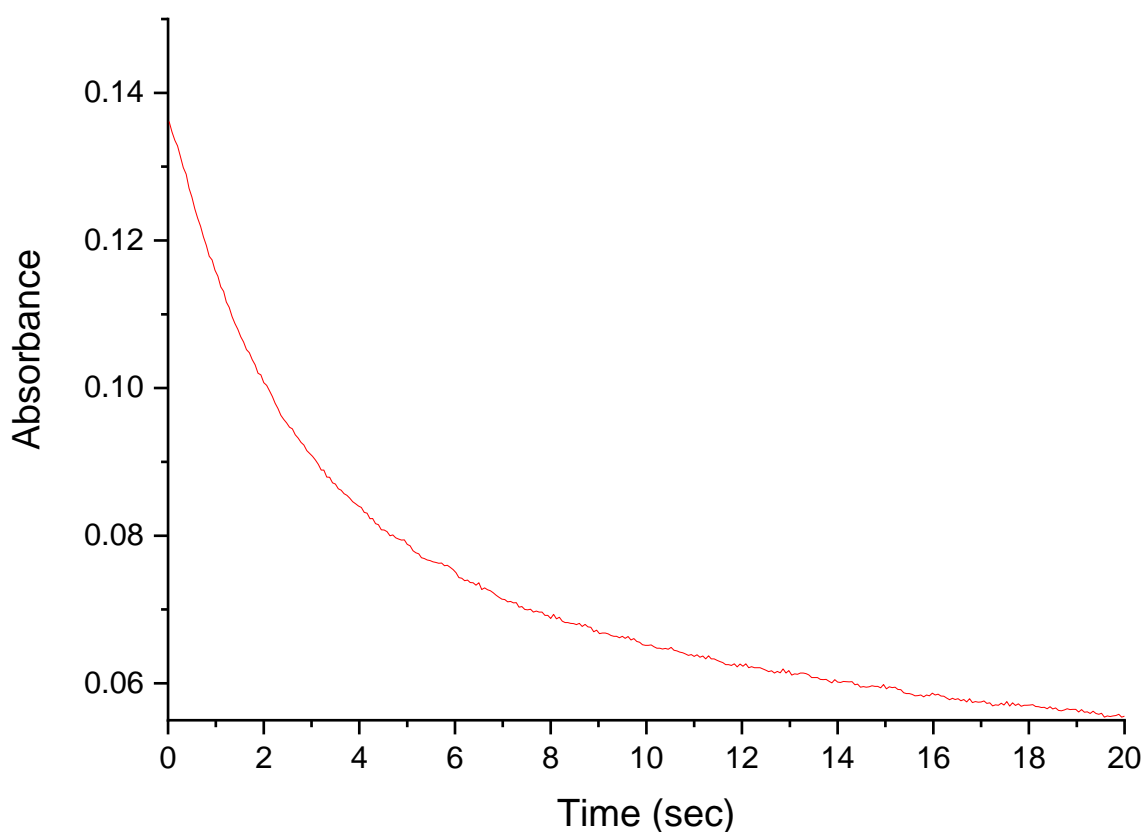


Figure 14: Typical kinetic trace showing the disappearance of TNB at 412 nm over time.

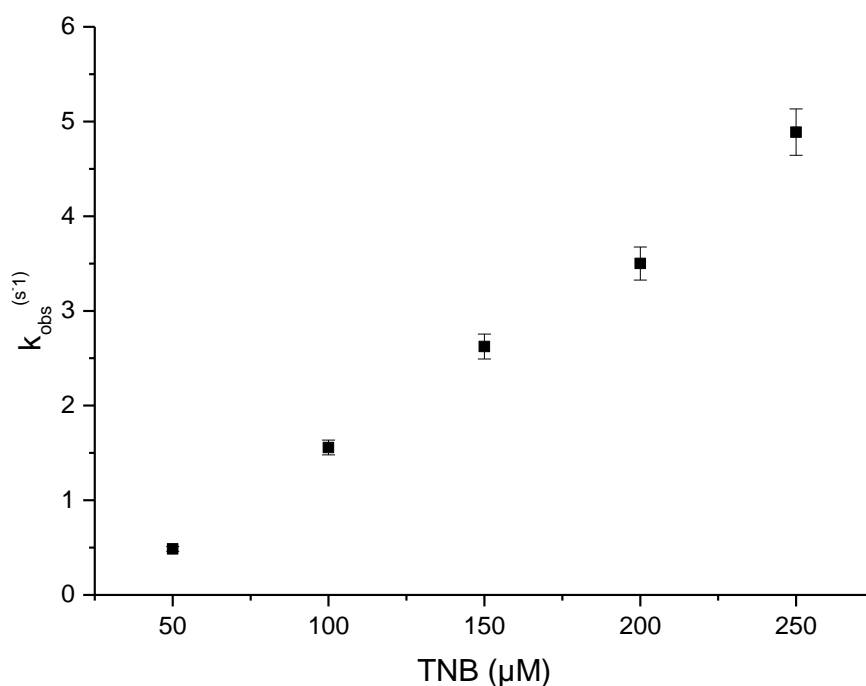


Figure 15: Linear plot for the observed rate constants k_{obs} following the disappearance of TNB at 412 nm. Results are represented as mean standard deviation. Some error bars are smaller than the size of the symbol.

3.5.2. Reaction of ICN with selected biological thiol groups

The rate of reaction of ICN with biologically important thiol groups including L-cysteine, cysteamine, *N*-acetyl-cysteine, L-cysteine methyl ester, penicillamine, glutathione and protein thiol BSA could not be measured accurately by direct method because these molecules do not have a clearly defined UV-vis spectra. The rates were thus determined by competition experiments using the rate constants determined above for TNB as a reference.

Competition experiments involved mixing a fixed amount of ICN with increasing concentration of each thiol at 22 °C. The kinetics of the reactions of ICN with each thiol was conducted in competition with TNB. Changes in absorbance at 412 nm arising from the reaction of ICN with TNB were used to measure the rate constants as these afforded measurements that are free from the interference of other absorbing species. The change in TNB absorbance obtained in the absence of any competing substrate ($Y_{\text{max}} = Y_{\text{max}}$), and in its presence ($Y_{\text{quench}} = Y_{\text{quench}}$) were measured at fixed time points for each thiol after a complete decay of TNB. Similar kinetic measurements were made by Skaff *et al* on the reaction of hypothiocyanite ion (OSCN^-) with low-molecular-mass thiols.⁸

The reaction of ICN with TNB in the absence of a competing thiol showed a dependence on ICN concentration. Close inspection of the spectral data indicate that no interference occurred from other absorbing species in the region of interest. Control experiments whereby DTNB (a disulfide of TNB) was reacted with ICN, showed no noticeable absorbance changes, ruling out the oxidation of DTNB by ICN as an alternative pathway for ICN consumption under the conditions of our experiments. Figure 16 illustrates typical time-resolved experiments for the reaction of TNB (50 μM) with ICN (10 μM) in the presence of increasing concentrations of cysteine at pH 7.4. Kinetic data was analysed according to the linear equation (10).

$$\frac{Y_{\text{max}} [\text{TNB}]}{Y_{\text{quench}}} = \frac{K_{\text{quench}} [\text{quench}]}{K_{\text{TNB}}} + [\text{TNB}] \quad (10)$$

The slope from the linear competition plot is equal to $k_{\text{quench}}/k_{\text{TNB}}$ and the y-intercept is given by the TNB concentration. Using the TNB rate constant obtained above, the second-order rate constant for the reaction of ICN with other thiols were determined and are presented in Table 2.

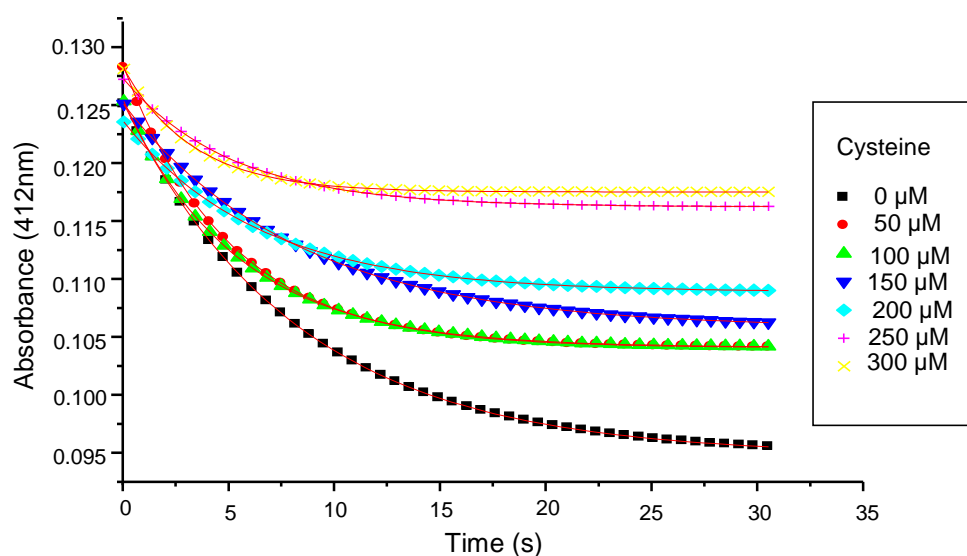


Figure 16: Kinetic traces showing the loss of TNB absorbance with increasing concentrations of the competing thiol L-cysteine at 412 nm.

Figure 17 shows error bars representing standard deviations from repeated experiments (see Figure 21 in appendix 1 for a typical linear competition plot) involving L-cysteine, which allowed for the second-order rate constant to be determined using the value of k_{TNB} measured above at pH 7.4.

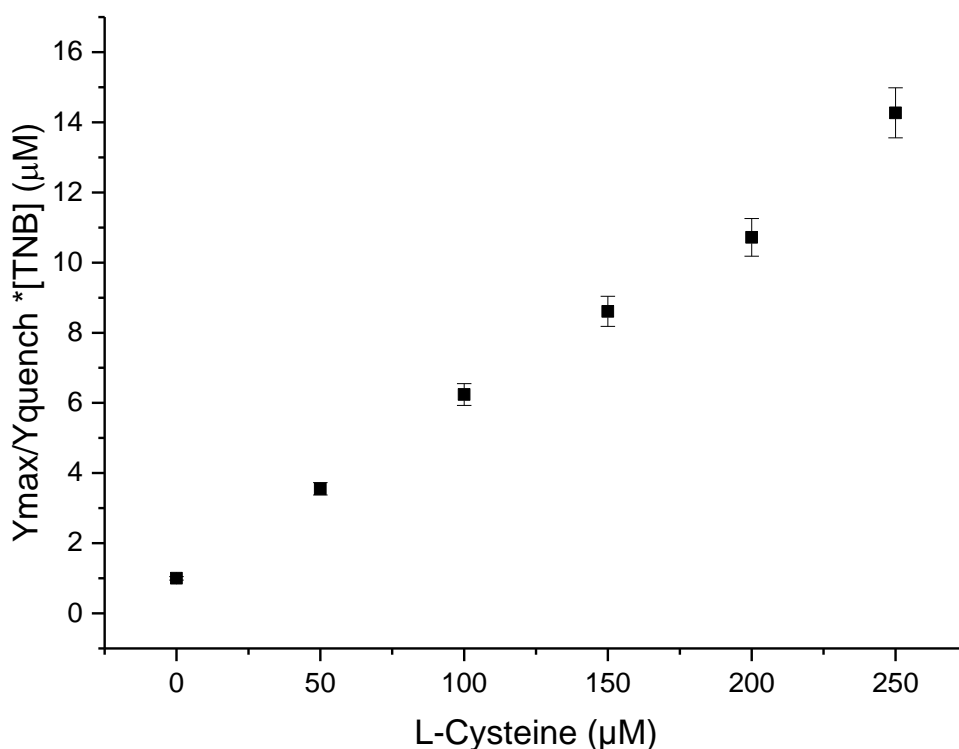
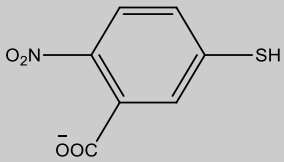
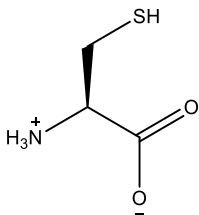

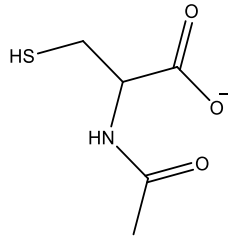
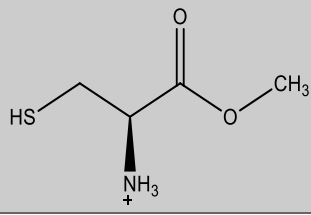
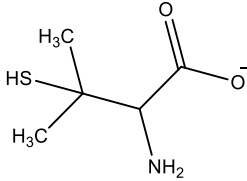
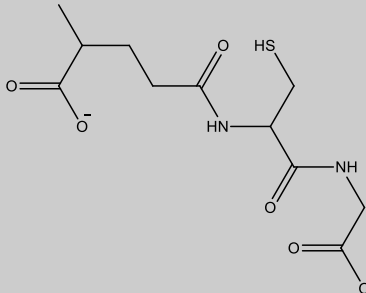


Figure 17: Plot of the linear analysis for the competitive kinetic data for L-cysteine with ICN at 412 nm. Result are represented as mean standard deviation. Some error bars are smaller than the size of the symbol.

The rate constants for the reactions of ICN with thiols have not been previously reported. Competition kinetic data for the reaction of ICN with other thiols is presented in Table 2. Rate constants varies over the range between $400 \text{ M}^{-1} \text{ s}^{-1}$ (penicillamine, pH 7.4) – $120000 \text{ M}^{-1} \text{ s}^{-1}$ (TNB, pH 6.0). The values of the rate constants are generally smaller than those observed for the reaction of OSCN^- with thiols. About 2 – 3 orders of magnitude difference exist between k_{OSCN} and k_{ICN} .

Table 2: The second-order rate constants in 0.1M phosphate buffer (pH 7.4) at 22 °C, for the reaction of ICN with low-molecular-mass thiols.

Substrate	Structure	pH	k_2 (ICN) ($M^{-1} s^{-1}$)
TBN		7.4	$2.1 (\pm 0.21) \times 10^4$
		6.7	$6.8 (\pm 0.2) \times 10^4$
		6.0	$1.2 (\pm 0.2) \times 10^5$
L-cysteine		7.4	$2.3 (\pm 0.1) \times 10^3$
Cysteamine		7.4	$8.6 (\pm 0.1) \times 10^2$
N-Acetyl-cysteine		7.4	$5.4 (\pm 0.2) \times 10^2$
L-Cysteine methyl ester		7.4	$7.9 (\pm 0.2) \times 10^2$
Penicillamine		7.4	$4.0 (\pm 0.1) \times 10^2$

GSH		7.4	$1.6 (\pm 0.2) \times 10^2$
		6.7	$2.5 (\pm 0.2) \times 10^2$
		6.0	$4.3 (\pm 0.2) \times 10^2$
Protein thiol BSA	-	7.4	$1.3 (\pm 0.7) \times 10^2$

3.5.3. Reaction of ICN with thiol-bearing proteins

Serum albumin is the most abundant and complex protein in the blood plasma of all vertebrates. It functions as a binder and transporter of numerous compounds including drugs and toxic waste. ¹¹ Bovine Serum Albumin (BSA), a large protein (65 kDa) derived from cows was selected in our investigation as a model for biological thiol-containing proteins. Kinetic measurements for the reactions of HOSCN with thiol-containing proteins have been conducted by Skaff *et al.* ⁸ The values obtained for four proteins including bovine serum albumin (BSA); creatine kinase (CK), β -lactoglobulin and β -L-crystallins lie with the range of $1.0 \times 10^4 - 7.0 \times 10^4 \text{ M}^{-1} \text{ s}^{-1}$. ⁸ Of the four proteins studied, BSA showed the highest reactivity with HOSCN an observation attributed to the highly exposed nucleophilic Cys³⁴ of BSA.

In this study, competition kinetic experiments were carried out using TNB (10 μM) to measure the rate constant for the reaction of ICN (10 μM) with BSA (50 – 250 μM). The reaction was followed by monitoring TNB absorbance loss at 412 nm with increasing BSA concentration. The likely site of ICN attachment is the free Cys³⁴,

which has a pKa of 8.5.⁸ The second-order rate constant of $1.3 \times 10^2 \text{ M}^{-1} \text{ s}^{-1}$ for the reaction of ICN with BSA at pH 7.4 was obtained. This value is comparable to those obtained for the reaction of ICN with free thiols as shown in Table 2. The second-order rate constant for the reaction of BSA with ICN is approximately 2.5 orders of magnitude smaller than with HOSCN.

3.5.4. Factors influencing the observed rate constants

3.5.4.1. pH dependence of ICN reactions

The rates of reactions of reduced glutathione (GSH) and TNB with ICN were measured in the range from pH 7.4 to 6.0. Lower (pH < 7.4) values were studied to mimic conditions found at sites of inflammation.⁹ Figure 18 shows an inverse relationship between the second-order rate constants and the pH for both GSH and TNB. The rate constants for TNB are 2-3 orders of magnitude larger than GSH at all pH values considered.

3.5.4.2. Dependence of the reactivity on thiol pKa

A plot of thiol pKa against the second-order rate constants (Figure 18) shows an inverse relationship. The observed increase in rate constants with decreasing thiol pKa is consistent with that reported for the reaction of thiols with HOSCN and taurine chloramine.^{8, 12} This trend indicates that the thiolate (RS^-) anion of each thiol is the reactive species. Only cysteine showed a slight deviation from this correlation. In the HOSCN study, this behaviour was displayed by cysteamine and attributed to its high net charge at pH 7.4.⁸ The reactivity of ICN with protein cysteine residues was

determined using BSA. The active site Cys³⁴ of BSA has a pKa of 8.5. The reactivity of ICN with BSA is of the same order of magnitude as the reaction with GSH and two order of magnitude lower than for the reaction of BSA with HOSCN. The high reactivity of BSA with HOSCN is attributed to the accessibility of the highly exposed Cys³⁴ residue in BSA. The inverse relationship observed between second-order rate constant and pKa suggests that other factors beyond pKa play a more important role on the reactivity.

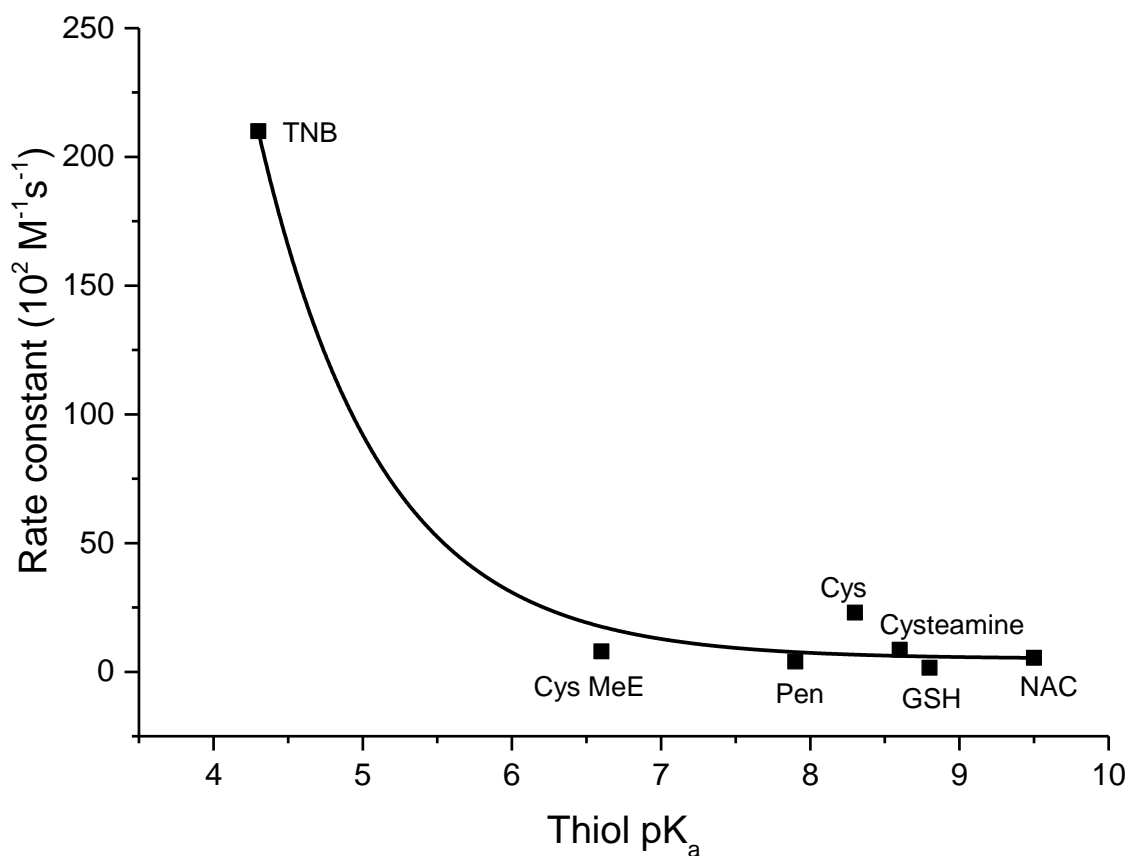


Figure 18: The linear plot showing the relationship between the second-order rate constants and thiol pKa for the reaction of thiols with ICN at pH 7.4. ⁸

3.6. Preliminary investigation of ICN antimicrobial activity

The presence of biofilm forming bacteria in nature remains a major challenge in both industry and medicine. Biofilms are microbial communities that adhere on surfaces thereby acting as diffusion barriers to approaching antimicrobial agents. The biofilm matrix insulates embedded bacteria from attack by antimicrobial agents such as ICN. The surge in reported cases of persistent bacterial infection is closely linked to the action of biofilms for example, in medicine chronic lung infection is caused by *Pseudomonas aeruginosa* biofilms in cystic fibrosis patients.¹³ In the food industry, *Penicillium expansum* is recognized as the main cause of decay on apples, pears and citrus fruits.³

The aim of this preliminary work was to develop capacity within our research group to conduct biological tests. Training for these tests was provided by Professor S Schmidh from the school of life science. The minimum inhibitory concentration of ICN was determined for *Escherichia coli* (*E. coli*) in liquid medium using previously described method.¹⁴ Several ICN solutions (5 – 50 μM) in phosphate buffer at pH 7.4 were tested against *E. coli* grown on agar plates. Following treatment, agar plates were incubated under dark conditions in the fumehood at room temperature for 30 days. Iodine/ iodide was also tested because it has antimicrobial properties.¹⁵ Enhanced inhibition (after 30 days) of bacterial growth even at 5 μM ICN solution was observed (Figure 19 (D₂)). In contrast, controls with glycerol and KI (5 μM) showed significant bacterial growth (Figure 19 B₂ and C₂ respectively).

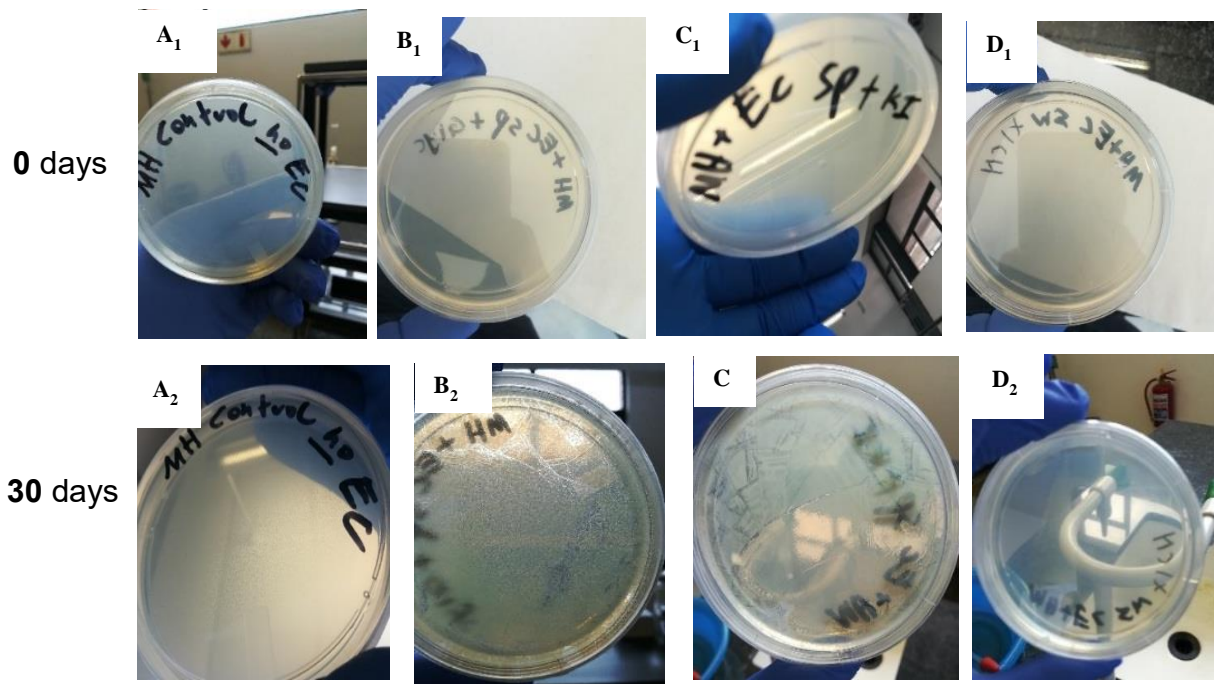


Figure 19: The agar plates taken before and after placing the plates under the fume hood cardboard. (A₁) Control with no *E. coli*; (B₁) with glycerol; (C₁) with KI; (D₁) with ICN. The agar plates taken after 30 days. (A₂) Control with no *E. coli*; (B₂) with Glycerol; (C₂) with KI; (D₂) with ICN.

3.7. Conclusion

Schlorke and co-workers have shown that ICN, a highly cytotoxic antimicrobial agent is produced by the LPO system in the presence of I^- and SCN^- .⁴ Furthermore, we have shown in this work that non-enzyme reactions of $OSCN^-$ with I^- produces I_2 which further reacts with SCN^- to produce ICN. This study reports for the first time the kinetic data for the reaction of ICN with selected low-molecular-mass thiols and protein thiol (BSA). Competition kinetics reveal that ICN reacts rapidly with thiols with second-order rate constants (in the range $10^2 - 10^5 \text{ M}^{-1} \text{ s}^{-1}$) that are approximately 2-3 orders of magnitude smaller than that for HOSCN. It is conceivable that the role played by these reactions is more prominent in locations such as the oral cavity where peroxidase, $OSCN^-$, I^- and SCN^- are all present in significant amounts. The data indicate that ICN likely releases its antimicrobial activity in part by targeting the bacterial thiol components in vivo.

3.8. Reference

1. Paquette, J.; Ford, B. L., Iodine chemistry in the + 1 oxidation state. I. The electronic spectra of OI^- , HOI , and H_2OI^+ . *Canadian journal of chemistry* **1985**, 63 (9), 2444-2448.
2. Wei, Y.-J.; Liu, C.-G.; Mo, L.-P., Ultraviolet absorption spectra of iodine, iodide ion and triiodide ion. *Guang pu xue yu guang pu fen xi= Guang pu* **2005**, 25 (1), 86.
3. Bafort, F.; Damblon, C.; Smargiasso, N.; De Pauw, E.; Perraudin, J. P.; Jijakli, M. H., Reaction product variability and biological activity of the lactoperoxidase system depending on medium ionic strength and pH, and on substrate relative concentration. *Chemistry & biodiversity* **2018**, 15 (3), e1700497.
4. Schlorke, D.; Flemmig, J.; Birkemeyer, C.; Arnhold, J., Formation of cyanogen iodide by lactoperoxidase. *Journal of inorganic biochemistry* **2016**, 154, 35-41.
5. Gerritsen, C. M.; Gazda, M.; Margerum, D. W., Non-metal redox kinetics: hypobromite and hypoiodite reactions with cyanide and the hydrolysis of cyanogen halides. *Inorganic Chemistry* **1993**, 32 (25), 5739-5748.
6. Bak, B.; Hillebert, A., Cyanogen Iodide- $[\text{NaCN}^+ \text{I}_2^-]$ $\text{ICN}^+ \text{NaI}$. *Organic Syntheses* **1952**, 32, 29-31.
7. Chadwick, B.; Long, D.; Qureshi, S., The Raman and infrared spectra of the dicyanoiodate (I) ion. *Journal of Raman Spectroscopy* **1980**, 9 (1), 1-4.
8. Skaff, O.; Pattison, D. I.; Davies, M. J., Hypothiocyanous acid reactivity with low-molecular-mass and protein thiols: absolute rate constants and assessment of biological relevance. *Biochemical Journal* **2009**, 422 (1), 111-117.
9. Jankowski, A.; Scott, C. C.; Grinstein, S., Determinants of the phagosomal pH in neutrophils. *Journal of Biological Chemistry* **2002**, 277 (8), 6059-6066.

10. Hackam, D. J.; Rotstein, O. D.; Zhang, W.-J.; Demaurex, N.; Woodside, M.; Tsai, O.; Grinstein, S., Regulation of Phagosomal Acidification Differential Targeting Of Na⁺/H⁺ Exchangers, Na⁺/K⁺-ATPases, And Vacuolar-Type H⁺-ATPases. *Journal of Biological Chemistry* **1997**, 272 (47), 29810-29820.
11. Peters Jr, T., *All about albumin: biochemistry, genetics, and medical applications*. Academic press: **1995**.
12. Peskin, A. V.; Winterbourn, C. C., Kinetics of the reactions of hypochlorous acid and amino acid chloramines with thiols, methionine, and ascorbate. *Free Radical Biology and Medicine* **2001**, 30 (5), 572-579.
13. Nickel, J.; Ruseska, I.; Wright, J.; Costerton, J., Tobramycin resistance of *Pseudomonas aeruginosa* cells growing as a biofilm on urinary catheter material. *Antimicrobial agents and chemotherapy* **1985**, 27 (4), 619-624.
14. Schlorke, D.; Atosuo, J.; Flemmig, J.; Lilius, E.-M.; Arnhold, J., Impact of cyanogen iodide in killing of *Escherichia coli* by the lactoperoxidase-hydrogen peroxide-(pseudo) halide system. *Free radical research* **2016**, 50 (12), 1287-1295.
15. Winkler, R., Iodine—a potential antioxidant and the role of Iodine/Iodide in health and disease. *Natural Science* **2015**, 7 (12), 548.

Appendix 1

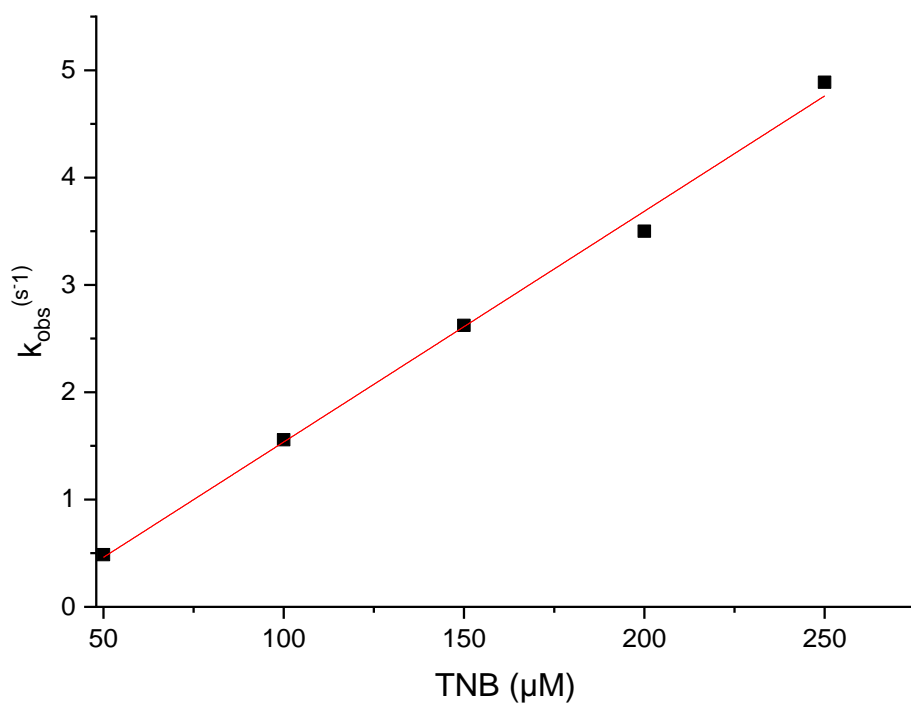


Figure 20: Linear plot for the observed rate constants k_{obs} following the disappearance of TNB at 412 nm.

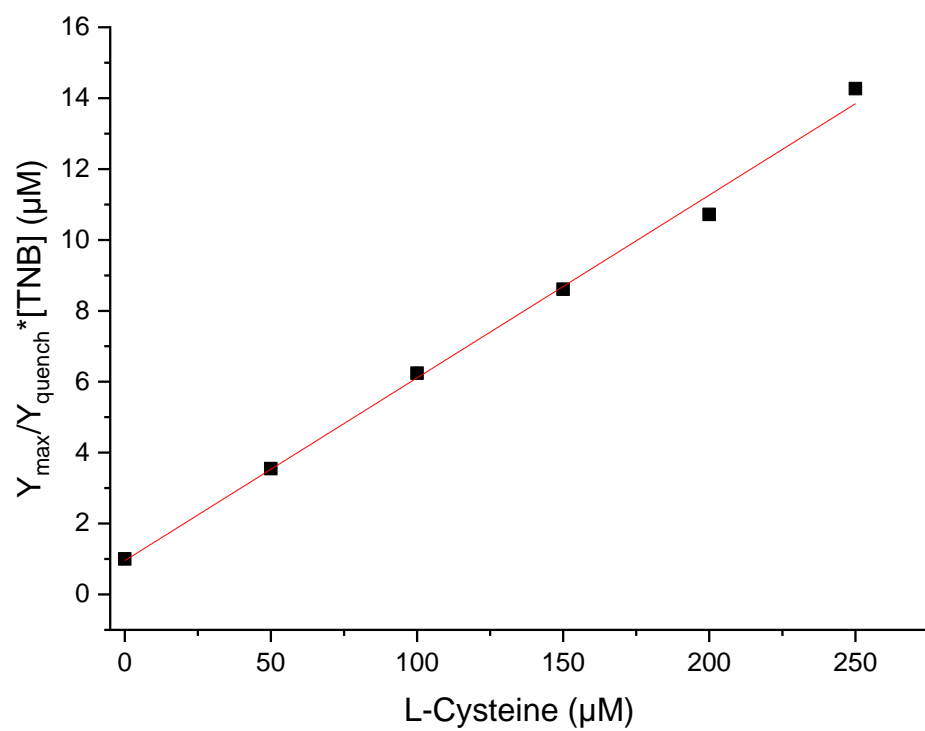


Figure 21: Plot of the linear analysis for the competitive kinetic data for L-cysteine with ICN at 412 nm.

